

1 **Carbon isotopes, stratigraphy and environmental change: the Middle/Upper**  
2 **Cambrian Positive Excursion (SPICE) in Port-au-Port Group, Western**  
3 **Newfoundland, Canada**

4 Rosalia Barili<sup>a,b</sup>, Joyce Neilson<sup>c</sup>, Alexander T. Brasier<sup>c</sup>, Karin Goldberg<sup>d</sup>, Tatiana Pastro Bardola<sup>a</sup>, Luiz  
5 Fernando De Ros<sup>a</sup>, & Melanie Leng<sup>e</sup>

6  
7 <sup>a</sup> Universidade Federal do Rio Grande do Sul – UFRGS  
8 Instituto de Geociências, Av. Bento Gonçalves, 9500, Porto Alegre, RS, Brazil  
9 rosalia.barili@gmail.com; lfderos@inf.ufrgs.br; tatiana.bardola@ufrgs.br

10  
11 <sup>b</sup> Instituto do Petróleo e dos Recursos Naturais – IPR  
12 Pontifícia Universidade Católica do Rio Grande do Sul – PUCRS  
13 Av. Ipiranga, 6681, prédio 96J. Porto Alegre, RS, Brazil  
14 rosalia.cunha@puccrs.br

15  
16 <sup>c</sup> University of Aberdeen.  
17 School of Geosciences, King's College, Aberdeen, UK  
18 j.neilson@abdn.ac.uk; a.brasier@abdn.ac.uk

19  
20 <sup>d</sup> Department of Geology, Kansas State University  
21 207 Thompson Hall, Manhattan, KS, 66506, USA  
22 kgoldberg@ksu.edu

23  
24 <sup>e</sup> NERC Isotope Geosciences Laboratory  
25 British Geological Survey, Keyworth, Nottingham NG12 5GG, UK  
26 mjl@bgs.ac.uk

27  
28 \*Corresponding author: rosalia.barili@gmail.com; Telephone: +55 51 99323 1060; +55 51 3219 0342  
29  
30

31 **Abstract**

32 In many basins, Upper Cambrian carbonate successions display intervals with a positive carbon  
33 isotope excursion (CIE) of up to +5‰. In North America, this marks the boundary between the  
34 Sauk II-III super-sequences. A Steptoean Positive Carbon Isotope Excursion (SPICE) locality  
35 previously identified in the Port-au-Port peninsula, western Newfoundland, has been revisited and  
36 an additional potential SPICE locality found. In both locations, a CIE is found to be associated with  
37 a prominent bioherm and sandstone layer within a sequence of carbonate rocks. At March Point,  
38 columnar stromatolites occur while at Felix Cove thrombolites can be seen. In the latter, the  
39 sandstone immediately overlies the thrombolites coincident with the CIE, while at March Point a  
40 dolomitized grainstone occurs above the stromatolites. The sandstone at this locality post-dates the  
41 CIE. Although lower than the SPICE in some localities, a positive CIE is present in both sections,  
42 March Point (+1.1 ‰) and Felix Cove (+1.8 ‰). Additionally,  $\delta^{13}\text{C}_{\text{org}}$  rises from -30.0 ‰ to -22.0  
43 ‰ at March Point, and from -27 ‰ to -24.0 ‰ at Felix Cove and, in accordance with previously  
44 published work, we suggest that this could be the SPICE. Comparison of the stratigraphy and  
45 petrography between the two localities suggest that both depositional and diagenetic factors could  
46 have influenced the nature of the interpreted SPICE in Newfoundland. It is also possible that the  
47 local carbon isotopic signature may have been influenced by a semi-restricted depositional and  
48 early diagenetic environment, related to the paleogeographic configuration, rather than the global  
49 marine excursion.

50 Keyword: SPICE, Port au Port Group, Stable Isotopes

## 51 **Introduction**

52 Upper Cambrian (Steptoean Stage) carbonate successions are found worldwide, including  
53 examples in North America, Siberia, Kazakhstan, China Australia and Oman (Figure 1), with a  
54 positive carbonate carbon isotope ( $\delta^{13}\text{C}_{\text{carb}}$ ) excursion (CIE) of up to +5‰, lasting nearly 4 Ma  
55 (Saltzman et al. 2000, 2004, Kouchinsky et al. 2008, Woods et al. 2011, Neilson et al. 2016). This  
56 excursion has also been observed in the  $\delta^{13}\text{C}$  of organic-rich ( $\delta^{13}\text{C}_{\text{org}}$ ) mudstones and shales  
57 (Ahlberg et al. 2009, Saltzman et al. 2011). This CIE was first reported from the John's Wash  
58 Limestone of Utah by Brasier (1993), followed by sections described in the House Range - Utah;  
59 McGill - Nevada; Wind Rover Range and Gros Ventre Range - Wyoming (Saltzman et al. 1995).  
60 The term Steptoean Positive Carbon Isotope Excursion (SPICE) was proposed by Saltzman et al.  
61 (1998), who suggested a global occurrence comparing data from South China, Kazakhstan,  
62 Australia and Laurentia (Shingle Pass, Nevada) (Saltzman et al. 2000). This positive carbon isotope  
63 excursion is coeval with a trilobite mass extinction horizon (Palmer 1965, Sepkoski 1982,  
64 Yochelson 1984, Saltzman et al. 1995, 1998, 2000, Bond and Grasby 2017). Saltzman et al. (2004,  
65 2011) and Bond and Grasby (2017) suggested that the positive excursion represents a perturbation  
66 in the global carbon cycle that occurs on the boundary between the Sauk II and Sauk III second  
67 order super-sequences from the Sauk megasequence (Sloss 1963).

68 Other CIE's of similar magnitude and duration have been described from the Late Ordovician, late  
69 Silurian, Upper Devonian, early Mississippian, and early late Permian (Gruszczynski et al. 1989;  
70 Brenchley 1994; Joachimski et al. 2002; Saltzman 2002, Saltzman et al. 2011). Each positive CIE  
71 may correspond to different causes, but in general they are thought to reflect an increased burial of  
72 isotopically lighter organic carbon (resulting in higher  $\delta^{13}\text{C}$  in the residual pool) related to  
73 increased organic productivity, with organic preservation due to high sedimentation rates and/or  
74 anoxic conditions (Arthur et al. 1987, Derry et al. 1992, Schidlowski 1992, Schrag et al. 2002).

75 The SPICE was first described in Western Newfoundland in the Petit Jardin Formation (Felix and  
76 overlying Man O' War members) at Felix Cove by Saltzman et al. (2004). In this unit,  $\delta^{13}\text{C}$  values  
77 of carbonates rise from -1‰ to 0‰ V-PDB, reaching a peak  $\delta^{13}\text{C}$  of +2.2‰ just above a quartz  
78 sandstone layer that marks the Sauk II – Sauk III boundary. Although the presence of an excursion  
79 has been reported in the Port au Port rocks (Saltzman et al. 2004), the magnitude of the SPICE  
80 excursion in the Petit Jardin Formation is smaller than observed around the world (Glumac and  
81 Walker 1998).

82 This raises questions about whether the presence of the global SPICE excursion in the Port au Port  
83 Peninsula rocks is real, or whether it is just a local environmental or diagenetic shift. In an attempt  
84 to address this issue, two Western Newfoundland stratigraphic sections were logged in detail,

85 followed by petrographic analysis of the carbonates, and  $\delta^{13}\text{C}$  analysis of both carbonate and  
86 organic carbon samples.

## 87 **Geologic Setting**

88 The study area is located on the southern coast of the Port au Port Peninsula, western  
89 Newfoundland (Figure 2). The SPICE was identified in Felix Cove (48°31'49.2"N / 58°47'12"E), a  
90 section previously studied by Saltzman et al. (2004) and another potential SPICE locality identified  
91 at March Point (48°30'42.1"N / 59°05'31.1"E),

92 The Port au Port Group forms part of the autochthonous Cambrian-Ordovician sequence of the  
93 tectono-stratigraphic Humber zone of the northern Appalachian orogeny (Williams 1976, 1979). It  
94 is interpreted as shallow-marine deposits from the outer part of a stable carbonate platform that  
95 surrounded the Iapetus Ocean (Williams 1976, 1979, Palmer and James 1979). These mixed  
96 carbonate-siliciclastic deposits record the gradual transition from early Cambrian siliciclastic  
97 deposition to predominantly carbonate sedimentation in the Early Ordovician (Chow 1985, Chow  
98 and James 1987b, Cowan and James 1993). The Group is composed of three formations, namely  
99 the March Point, Petit Jardin (Cape Ann, Campbells, Big Cove, Felix and Man O' War Members)  
100 and Berry Head Formations.

101 Transgressive-regressive Grand Cycles are identified through the Port au Port Group (Chow 1985,  
102 Chow and James 1987a, 1987b) (Figure 3). The marine transgression at the beginning of the Grand  
103 Cycles resulted in a shallow subtidal-intertidal environment, where relatively muddy carbonates  
104 were deposited (shaley packages and parted limestone; Chow and James 1987b). These deposits  
105 pass upwards into more open marine oolitic shoals, probably deposited near the platform edge  
106 (carbonate packages; Chow and James 1987b). As sea level dropped at the top of the cycles, the  
107 environment returned to a more restricted water circulation situation, although according to Chow  
108 and James (1987b) extensive evidence of subaerial exposure at the top of cycle B is absent. Carbon  
109 isotope data, previously collected in the Port au Port Group at Felix Cove, show a strong positive  
110  $\delta^{13}\text{C}_{\text{carb}}$  excursion between the Felix and Man O' War Members (Figure 1), which has been  
111 interpreted as the SPICE (Saltzman et al. 2004).

## 112 **Methodology**

113 The field work was performed along two main outcrops on the Port au Port Peninsula – March  
114 Point and Felix Cove. Detailed sedimentological logging on a cm scale (1:50) and systematic  
115 sampling was carried out at 1m resolution, from the base of accessible units in the Petit Jardin  
116 Formation to the top of each exposed Petit Jardin or Berry Head Formation section. The  
117 stratigraphic section logged in the March Point locality (MP) was 270m thick, and in the Felix

118 Cove locality (FC), 40m thick. A third outcrop was found, in which the diagnostic  
119 sedimentological characteristics of the SPICE layer in the Port-au-Port peninsula are exhibited  
120 (West Felix Cove 48°31'51.6"N / 58°47'49.1"E), but logging was not carried out at this location.

121 Representative layers were selected for thin sections (March Point: 45; Felix Cove: 8), carbonate  
122  $\delta^{13}\text{C}$  and  $\delta^{18}\text{O}$  analyses (March Point: 41; Felix Cove: 16), and organic carbon ( $\delta^{13}\text{C}_{\text{org}}$ ) (March  
123 Point: 14; Felix Cove: 4). Polished thin sections were prepared at the Mineral and Rock Analyses  
124 Laboratory (LAMIR) at the Universidade Federal do Paraná (UFPR) and at Petrografia BR, after  
125 impregnation with blue resin for porosity identification. Petrographic analysis was performed at the  
126 Universidade Federal do Rio Grande do Sul (UFRGS). For carbonate identification, the thin  
127 sections were stained with a solution of alizarin red.

128 Carbonate stable isotope ( $\delta^{13}\text{C}_{\text{carb}}$  and  $\delta^{18}\text{O}_{\text{carb}}$ ) analysis was carried out at LAMIR/UFPR in Brazil  
129 and at the BGS in the UK. For isotope analyses, carbonate samples were collected using a  
130 microdrill (0.5mm diamond drill), in order to avoid mixing of primary and diagenetic constituents  
131 whenever possible. At LAMIR, the amount of material drilled was around 0.3 mg, while a larger  
132 amount of powder was required by the BGS for the analysis (10mg). At LAMIR, the isotope ratios  
133 were determined using a GasBench II attached to a Thermo Scientific Delta Advantage continuous  
134 flow isotope ratio mass spectrometer, following the Spötl and Vennemann (2003) and Paul and  
135 Skrzypek (2007) routine with a reproducibility  $<0.1\%$  ( $1\sigma$ ). At BGS, isotopic analysis was carried  
136 out using a vacuum extraction technique and a VG Optima mass spectrometer with overall  
137 analytical reproducibility better than  $<0.1\%$  ( $1\sigma$ ) for  $\delta^{13}\text{C}_{\text{carb}}$  and  $\delta^{18}\text{O}_{\text{carb}}$ . The main difference in  
138 the carbonate isotope methodology of the two laboratories is the time of carbonate-acid reaction. At  
139 the BGS a quick reaction at low temperature ( $16^\circ\text{C}$ ) was performed over two hours in order to  
140 release  $\text{CO}_2$  from calcite with minimal contribution from any  $\text{CO}_2$  derived from secondary  
141 dolomite. However, at LAMIR, the time taken for reaction was between one to two hours at a  
142 temperature of  $72^\circ\text{C}$ . The isotope composition of samples is reported in the standard  $\delta$  notation,  
143 defined as the relative difference, in parts per thousand (‰) without any further conversion. Each  
144 laboratory used their own in house standards previously calibrated to Vienna Pee Dee Belemnite  
145 (V-PDB).

146 For organic carbon isotope ( $\delta^{13}\text{C}_{\text{org}}$ ) analysis at the BGS, the samples were reacted with 5% HCl  
147 overnight to remove carbonate, and dried down at  $40^\circ\text{C}$ . After being cleaned, homogenized, and  
148 dried, c. 15–25 mg of decarbonized sediment were used for determination of carbon isotope ratios  
149 using a carbon isotopic ratio Carlo Erba 1500 on-line to a VG TripleTrap (with a secondary  
150 cryogenic trap for very low carbon content samples) and Optima dual-inlet mass spectrometer.  
151  $\delta^{13}\text{C}_{\text{org}}$  values were calculated to the V-PDB scale using a within-run laboratory standard (BROC1)

152 calibrated against NBS-19 and NBS-22. Replicate analysis of well-mixed samples embraces a  
153 precision of  $\pm <0.1\text{‰}$  ( $1 \sigma$ ).

## 154 **Results**

155 The stratigraphic interval that comprises the purported SPICE in Felix Cove (as identified by  
156 Saltzman, 2004, at 22.5 m, Figure 4a) comprises several sets of fining-upward oolitic grainstones  
157 (20-40 cm thickness), followed by a layer of pillow-shaped thrombolite, around 25 cm thick, with a  
158 clotted center tending to a more regular shape at the edges (Figure 4b). The sedimentary layers that  
159 underly the thrombolite layer contain trilobites of the *Crepicephalus* Zone (*Terranovella dorsalis*  
160 and *Crepicephalus iowensis* in the FC1 and FC2 collections of Westrop, 1992). Westrop (1992)  
161 also records the occurrence of the trilobite *Dytremacephalus strictus* in the thrombolite layer itself  
162 (R. Levesque, Geological Survey of Canada, location 96635), indicating that it belongs to the  
163 *Aphelaspis* Zone (Figure 3). These bioherms are overlain by a thin glauconitic sandstone layer (~25  
164 cm thickness) before returning upwards to grainstones and parted limestone sets. These sets show  
165 different degrees of dolomitization, but it is still possible to identify primary constituents.  
166 Saltzman et al. (2004) note that Elvinia Zone fauna (A.R. Palmer, Institute for Cambrian Studies  
167 collection ICS-1406) were found approximately 8 m above the quartz sandstone. The trilobite data  
168 confirms the CIE as being the SPICE. A similar lithological succession is observed in West Felix  
169 Cove (Figure 4c).

170 In the March Point section, the interval that comprises the positive carbon excursion, between  
171 222m and 226 m, consists of a layer of columnar stromatolites (Figure 4d), around 20 cm thick,  
172 either forming as separated columns or laterally continuous mats. These are overlain by a thin  
173 dolomitized glauconitic grainstone, 20 cm thick (Figure 4e). A meter-thick glauconitic, fine-  
174 grained sandstone (Figure 4f) occurs 3-4 m above. Below the stromatolite layer, the oolitic  
175 grainstone sets are extensively dolomitized. No well constrained faunal information is available for  
176 this layer.

177 The uncompacted bioclastic sandstone that overlies the bioherms in Felix Cove is cemented by  
178 calcite with very minor replacive dolomite (Figure 5a) although in West Felix Cove the dolomite  
179 content is considerably higher, showing small relict calcite areas (pinkish stain) (Figure 5b). Quartz  
180 grains are well rounded and well sorted, medium coarse – coarse sand, with 465  $\mu\text{m}$  diameter  
181 average (Table 1). The glauconitic grainstone that overlies the stromatolites at March Point is  
182 extensively dolomitized (Figure 5c) including the glauconite peloids (Figure 5d). The glauconitic  
183 sandstone layer, 3-4 m above it, contains very poorly sorted, sub-rounded to angular silt to medium  
184 sand grains (89  $\mu\text{m}$  diameter average) which is also partially cemented by dolomite (Figure 5e and  
185 f) and is very compacted. The sets of oolitic grainstones that underlie the potential SPICE layer in

186 March Point are extensively dolomitized although the ooids outlines may be partially preserved  
 187 (Figure 6a-c). For several meters above the potential SPICE layer, carbonate-clastic sandstones  
 188 (composed of quartz grains and carbonate particles) occur (Figure 6d), replaced by dolomite.

189 The isotope data ( $\delta^{13}\text{C}_{\text{carb}}$ ,  $\delta^{18}\text{O}_{\text{carb}}$ ,  $\delta^{13}\text{C}_{\text{org}}$  and %C) analysis for the March Point section are  
 190 presented in Table 2 and Figure 7. The  $\delta^{13}\text{C}_{\text{org}}$  data are relatively stable below the base of the Felix  
 191 Member, with values between  $-29.5\text{‰}$  and  $-24.8\text{‰}$ . Above this point, however, the values become  
 192 more variable, between  $-30\text{‰}$  and  $-21.3\text{‰}$ , showing a general enrichment in  $^{13}\text{C}$  organic carbon up  
 193 section, with a maximum within the Felix Member. The total organic carbon level (%C), however,  
 194 is generally very low, ranging between 0.04% and 0.3%, except for layers at 170 and 180m, with  
 195 1.9% and 2.1% respectively. The  $\delta^{13}\text{C}_{\text{carb}}$  data show significant depletion at the top of the  
 196 Campbells Member ( $-4.1\text{‰}$ ), and a maximum ( $+1.1\text{‰}$ ) at the boundary between the Felix and Man  
 197 O' War Members. Above this, the  $\delta^{13}\text{C}_{\text{carb}}$  general trend is towards lower values between  $-2$  and  $-$   
 198  $1\text{‰}$ . In the March point section the best defined carbonate carbon excursion occurs over a thickness  
 199 of approximately 5 m (Figure 7).  $\delta^{18}\text{O}_{\text{carb}}$  values are not directly related to the  $\delta^{13}\text{C}_{\text{carb}}$  values ( $r^2 =$   
 200  $0.21$ ,  $n = 41$ ), although they show similar trends. However,  $\delta^{18}\text{O}_{\text{carb}}$  becomes less variable in the  
 201 Felix Member, showing a more positive peak, around  $-4.5\text{‰}$ , which coincides with the positive  
 202 shift in  $\delta^{13}\text{C}_{\text{carb}}$  at the boundary between the Felix Cove and Man O' War Members.

203 In the Felix Cove section, only part of the Petit Jardin Formation is exposed, starting within the  
 204 Felix Member. The  $\delta^{13}\text{C}_{\text{carb}}$ ,  $\delta^{18}\text{O}_{\text{carb}}$ ,  $\delta^{13}\text{C}_{\text{org}}$  and %C data are given in Table 2 and Figure 8. Near  
 205 the lowermost part of the outcrop exposed in the Felix Member, the  $\delta^{13}\text{C}_{\text{carb}}$  value is around  $-2.0\text{‰}$ ,  
 206 reaching a high of  $+1.8\text{‰}$  near to the transition between the Felix and Man O' War Members  
 207 (Figure 8). This section corresponds to the same interval studied by Saltzman et al. (2004). The  
 208 data present a general upward increase in  $\delta^{13}\text{C}_{\text{carb}}$  values (Figure 8). Compared to  $\delta^{13}\text{C}_{\text{carb}}$ , the  
 209  $\delta^{18}\text{O}_{\text{carb}}$  data shows a relatively stable trend, as observed for the Felix Member in the March Point  
 210 section, with a negative trough (though only of one data point) of  $-9.0\text{‰}$  just before an interval of  
 211 higher values that reach  $-5.4\text{‰}$ . A weak correlation between  $\delta^{13}\text{C}_{\text{carb}}$  and  $\delta^{18}\text{O}_{\text{carb}}$  occurs for the  
 212 Felix Cove section ( $r^2 = 0.57$ ,  $n = 16$ ). As in the March Point section, %C is low, ranging between  
 213 0.04% and 0.17%. The stratigraphic thickness of the excursion upwards from 22.25 m, is about 15  
 214 m (Figure 8).

## 215 Discussion

216 In the Port au Port Peninsula, particular lithologies were found to be related to the peak  $\delta^{13}\text{C}$  values  
 217 in outcrop. This positive  $\delta^{13}\text{C}$  excursion was observed and identified by Saltzman et al. (2004) at  
 218 Felix Cove and, based on trilobite data presented by Westrop (1992), identified as the SPICE. The  
 219 positive  $\delta^{13}\text{C}$  excursion occurs at a time when there was an influx of glauconitic quartzose sand

220 believed to be as a result of a decrease in water depth (regression). This was followed by a rise in  
221 sea level and deepening (Saltzman et al. 2004), reflected in the resumption of carbonate deposition.  
222 Detailed logging of the SPICE section at Felix Cove has shown that the positive peak is  
223 characterized by a lithological sequence of bioherms, overlain by glauconitic sand rich layers, also  
224 observed by Saltzman et al. (2004). A very similar lithological sequence has also been identified  
225 during this study approximately 0.8 km west of Felix Cove (West Felix Cove) although limited  
226 data is available.

227 In the March Point section (approximately 25 km further west, Figure 2), a similar lithological  
228 sequence of bioherms and glauconitic sandstone occur in the interval and is accompanied by a  
229 positive carbon isotope excursion (Figure 7). No biostratigraphic data are available for the upper  
230 part of the Felix Member. Westrop (1992) provides data for the underlying Big Cove Member but  
231 this lies well below where the SPICE would be expected in that section.

232 Although there are similarities in the lithological sequence between these localities, there are also  
233 differences. Folk (1951) suggested that textural and compositional maturity of the sediment are  
234 products of the degree of reworking, energy and distance of transport. The fine, poorly sorted,  
235 slightly immature sandstones at March Point (Figure 5e and f, Table 1) contrast with the “clean”,  
236 coarse and mature sandstone observed at Felix Cove (Figure 6a and b). Also, the position of the  
237 distinctive glauconitic sandstone is different. At Felix Cove it directly overlies the thrombolites  
238 while at March Point it occurs 3-4m above it. At March Point, the stromatolite is overlain by a  
239 dolomitized glauconitic grainstone prior to deposition of the glauconitic sandstone. Moreover, even  
240 though it is unlikely that the morphology of specific microbial buildups was related to particular  
241 environments, lateral differences do exist. The bioherm morphology at March Point comprise  
242 columnar stromatolites, (Figure 4e) while thrombolites are observed in this layer at Felix Cove  
243 (Figure 4a-c). The interval at March Point can therefore only be identified as a potential SPICE  
244 locality.

245 The Felix Cove section indicates that the lead up to the SPICE occurred in a shallow marine  
246 environment, with bioclastic grainstone shoals (e.g. echinoderms) and bioherms. The influx of  
247 coarse, well rounded, quartz sandstone marks the base of the positive carbon excursion and start of  
248 a regression. The sandstone layer is followed by several sets of fining upward oolitic bioclastic  
249 grainstones, up to the Felix/Man O' War member transition, where parted limestone and shale  
250 become abundant. These deposits have been interpreted by Chow and James (1987b) as subtidal to  
251 intertidal. Comparatively, in the March Point section the positive carbon excursion (potential  
252 SPICE) occurs within a set of a glauconitic grainstones. The fine, angular, carbonate-clastic  
253 sandstone occurs a few metres above the peak of the positive  $\delta^{13}\text{C}_{\text{carb}}$  excursion rather than at its  
254 beginning, near to the transition between Felix and Man O' War members. This suggests that the



255 sandstones at the two locations are diachronous and may have been deposited in different  
256 environments with the start of the regression being slightly later at March Point than at Felix Cove.

257 While the SPICE interval is 200 m thick in Nevada (Saltzman et al. 1998) and 80 m in the Southern  
258 Appalachians (Glumac and Walker 1998), it is only 15 m thick in the Felix Cove section and the  
259 potential SPICE only 5 m thick in the March Point section (Figure 9). This has already been noted  
260 by James and Stevens (1986), who found a thickness of less than 20 m, similar to our observations  
261 at Felix Cove. However we observed a much thinner interval in the March Point section.

262 Additionally, the  $\delta^{13}\text{C}_{\text{carb}}$  of the SPICE has a relatively lower magnitude than observed in other  
263 suggested localities around the world. Globally, the SPICE is described as a  $\delta^{13}\text{C}_{\text{carb}}$  positive shift  
264 of around +5‰ (Saltzman et al. 2000, 2004, Kouchinsky et al. 2008, Woods et al. 2011) in  
265 carbonates. The results presented here reach a  $\delta^{13}\text{C}_{\text{carb}}$  peak of about +1.13 ‰ for the March Point  
266 section and +2.2 ‰ (Saltzman et al. 2004), and +1.8 ‰ (this work) for the Felix Cove section, with  
267 an average shift of about +2 ‰, half of the typical global value. There are other locations which  
268 have lower values, for example in the Southern Appalachians and South China (~+3‰; Fan et al.  
269 2011).

270 At March Point, dolomitisation is significant in the immediate lead up to and around the potential  
271 SPICE interval and this may have affected the isotopic results. To minimize the effect of this, the  
272 data around the potential SPICE interval itself were collected at the BGS (Figure 7) using a quick  
273 acid reaction time. This was performed over two hours at low temperature (16°C) to release  $\text{CO}_2$   
274 mainly from calcite and minimize the contribution from dolomite. At March Point, the higher  
275  $\delta^{13}\text{C}_{\text{carb}}$  values are accompanied by an increase in  $\delta^{18}\text{O}_{\text{carb}}$  (up to c. -4‰, Figure 7). A similar  
276 pattern in  $\delta^{18}\text{O}_{\text{carb}}$  values is recorded from early dolomites in the Lower-Middle Triassic Moenkopi  
277 Formation (Marenco et al. 2008). The early, relatively heavy Moenkopi Formation dolomites were  
278 contemporaneous with inner-middle shelf limestones which showed much lighter  $\delta^{18}\text{O}_{\text{carb}}$  values of  
279 -9 to -6‰. The  $\delta^{18}\text{O}_{\text{carb}}$  data observed here may therefore reflect a contribution from early  
280 dolomitisation which may be more likely to have retained the original carbon isotopic signature due  
281 to a lack of subsequent recrystallisation.

282 Considering the wider effects of diagenesis, the more negative  $\delta^{18}\text{O}_{\text{carb}}$  data observed in both  
283 sections could be the result of burial and interaction with hot or meteoric diagenetic fluids (Scholle  
284 1977, Moore 2002). Thus, the large depletion in  $\delta^{18}\text{O}_{\text{carb}}$  values (down to -9‰, Figures 7 and 8)  
285 could be interpreted as a diagenetic effect, marked by resetting of the original isotope ratios (Brand  
286 and Veizer 1980). Despite different diagenetic patterns around the SPICE and potential SPICE  
287 intervals, both sections show similar  $\delta^{18}\text{O}$  values at that level (between -4.5 and -5.75 ‰, Figures  
288 7 and 8). These values are heavier than most of the samples that lie stratigraphically below or

289 above the potential SPICE at March Point. This may suggest that the original signature has been  
290 preserved better around the SPICE and potential SPICE interval.

291 A positive excursion was observed in  $\delta^{13}\text{C}_{\text{org}}$  data from Avalonia (Woods et al. 2011), Australia,  
292 China and North America (Iowa) (Saltzman et al. 2011). In Newfoundland this is also observed  
293 although an offset between  $\delta^{13}\text{C}_{\text{org}}$  and  $\delta^{13}\text{C}_{\text{carb}}$  occurs in the March Point section and, to a lesser  
294 degree, in the Felix Cove section (Figure 10). The isotope offset between  $\delta^{13}\text{C}_{\text{org}}$  and  $\delta^{13}\text{C}_{\text{carb}}$  curves  
295 has been noted previously in Queensland, Australia and Iowa, USA by Saltzman et al. (2011).  
296 There,  $\delta^{13}\text{C}_{\text{org}}$  was found to track the  $\delta^{13}\text{C}_{\text{carb}}$  curve on the rising limb, with  $\delta^{13}\text{C}_{\text{org}}$  shifting back to  
297 lighter values before peak SPICE in the inorganic data. Although the pattern is clear at March  
298 Point, the reduced thickness of the Felix Member exposed at Felix Cove makes it more difficult to  
299 identify there. The highly variable trend in  $\delta^{13}\text{C}_{\text{org}}$  below the potential SPICE at March Point is  
300 most likely due to the low %C values in most of the samples.

301 The SPICE is a global phenomenon and represents the characteristics of open ocean seawater at  
302 that time. However, as shown earlier, the Petit Jardin Formation was deposited in a more marginal  
303 marine environment (Chow and James, 1987b) rather than open marine. Gilleaudeau and Kah,  
304 (2013) have shown that carbonates deposited in epicratonic seas are typically 2-4 ‰ lighter in  $\delta^{13}\text{C}$   
305 than those deposited in open-marine pericratonic environments. Gilleaudeau and Kah (2013)  
306 suggest that general mechanisms for this include  $^{13}\text{C}$ -depletion due to marine upwelling,  $^{13}\text{C}$ -  
307 depletion from terrigenous plant material (even in pre-Silurian environments from early  
308 bryophytes) or  $^{13}\text{C}$ -depletion from in situ organic remineralisation.

309 Local tectonics may also have played a part in reducing the extent of the CIE. It has been suggested  
310 that local tectonics influenced the sedimentation patterns observed in the Port-au-Port peninsula in  
311 the inner flexural wedge of the Laurentian cratonic margin (Cowan and James, 1993; Lavoie et al,  
312 2012). Even for relatively adjacent locations such as Felix Cove and March Point (c. 25 km apart),  
313 local tectonics could have accounted for the variations in input and timing of the clastics observed  
314 related to the SPICE and potential SPICE (Figure 9) and could have generated local, more  
315 restricted environments. These environments would have had differences in energy (Knight and  
316 Boyce 2009) which again could have affected the geochemical signature (Gilleaudeau and Kah,  
317 2013).

318 As the platforms evolved due to closure of Iapetus, Western Newfoundland and its surroundings,  
319 located in southern Laurentia, became progressively more restricted whereas SPICE outcrops  
320 situated on the west/northwest of Laurentia maintained open circulation (Figure 11). Likewise,  
321 deposition in the southern Appalachians also occurred in a similar progressively restricted  
322 environment. The CIE in the southern Appalachians, like the SPICE and potential SPICE in  
323 Newfoundland, is thinner with a reduced magnitude.

324 The isotopic signal observed in the Petit Jardin Formation therefore, could reflect superposition of  
325 a regional and local signature onto ocean chemistry as a result of semi-restricted/restricted water  
326 circulation in the Newfoundland area due to SL changes and closure of the Iapetus Ocean (Cowan  
327 and James 1993, Patterson and Walter 1994, Saltzman et al. 2004). Hence, despite recording a  
328 positive excursion plausibly related to the SPICE, the Petit Jardin Formation may have imparted its  
329 own isotopic signature onto the SPICE, driven by local tectonic, sedimentary and diagenetic  
330 processes.

### 331 **Conclusions**

332 Two upper Cambrian sections in the Port-au-Port peninsula, Western Newfoundland have been  
333 studied and compared in detail (March Point and Felix Cove) These are predominantly carbonate in  
334 lithology but contain specific sandstone horizons that occur in close proximity to bioherms. At  
335 March Point, this bioherm is of stromatolitic character and a poorly sorted glauconitic sandstone  
336 layer occurs 3-4 m above it. At Felix Cove, the bioherm is thrombolitic and directly overlain by a  
337 coarse glauconitic sandstone. The sandstones are therefore diachronous.

338 Carbon isotope data (from both carbonate carbon and organic carbon) show a positive excursion (at  
339 the level which marks the boundary between Sauk II and III. Saltzman et al. (2004) presented data  
340 for the section at Felix Cove which has been dated by trilobite fauna and identified as the SPICE.  
341 New data from a potential SPICE horizon at March Point is presented in this work but no  
342 biostratigraphic data are available.

343 The  $\delta^{13}\text{C}_{\text{carb}}$  excursion presented here and by Saltzman et al. (2004) is reduced in magnitude  
344 compared to other global occurrences of the SPICE. This may be driven by local tectonic,  
345 sedimentary and/or diagenetic processes. A restricted environment would result in a less well  
346 developed excursion rather than the expected global CIE due to ocean chemistry. The stratigraphic  
347 and isotope variations observed in the Port-au-Port peninsula associated with the SPICE suggest  
348 that local as well as global conditions were important in determining its character.

### 349 **Acknowledgments**

350  
351 This work is a part of the PhD of the first author, developed at Universidade Federal do Rio Grande  
352 do Sul (UFRGS) and University of Aberdeen (UoA). The authors gratefully acknowledge support  
353 from Shell Brasil through the “BG05: UoA-UFRGS-SWB Sedimentary Systems” project at  
354 UFRGS and the strategic importance of the support given by ANP through the R&D levy  
355 regulation. BGS and LAMIR staffs are also acknowledged for assisting with stable isotope  
356 analysis. We also would like to thank Dr. Duncan McIlroy for all his help during the field work, and

357 Dr. Marc Laflamme, Dr. Pedro Jose Marengo and an anonymous reviewer for their help in  
358 improving the manuscript.

### 359 **References**

- 360 Ahlberg, P., Axheimer, N., Babcock, L.E., Eriksson, M.E., Schmitz, B., and Terfelt, F. 2009.  
361 Cambrian high-resolution biostratigraphy and carbon isotope chemostratigraphy in Scania,  
362 Sweden: First record of the SPICE and DICE excursions in Scandinavia. *Lethaia*, **42**: 2–16.
- 363 Arthur, M.A., Schlanger, S.O., and Jenkyns, H.C. 1987. The Cenomanian-Turonian Oceanic  
364 Anoxic Event, II. Palaeoceanographic controls on organic-matter production and  
365 preservation. Geological Society, London, Special Publications, **26**: 401–420.
- 366 Blakey, R. 2016. Deep Time Maps. Available from <https://www2.nau.edu/rcb7/RCB.html>.
- 367 Bond, D.P.G., and Grasby, S.E. 2017. On the causes of mass extinctions. *Palaeogeography,*  
368 *Palaeoclimatology, Palaeoecology*, **478**: 3–29.
- 369 Brand, U., and Veizer, J. 1980. Chemical Diagenesis of a Multicomponent Carbonate System-1:  
370 Trace Elements. *SEPM Journal of Sedimentary Research*, **Vol. 50**.
- 371 Brasier, M.D. 1993. Towards a carbon isotope stratigraphy of the Cambrian System: potential of  
372 the Great Basin succession. Geological Society, London, Special Publications, **70**: 341–350.
- 373 Brenchley, P.J. 1994. Bathymetric and isotopic evidence for a short-lived late Ordovician  
374 glaciation in a greenhouse period. *Geology*, **22**: 295–298.
- 375 Chow, N. 1985. Sedimentology and diagenesis of Middle and Upper Cambrian platform carbonates  
376 and siliciclastics, Port au Port Peninsula, western Newfoundland. Thesis (Unpublished).
- 377 Chow, N., and James, N. 1987a. Depletion of  $^{13}\text{C}$  in seawater  $\Sigma\text{CO}_2$  on modern carbonate  
378 platforms: Significance for the carbon isotopic record of carbonates. *Journal of Sedimentary*  
379 *Research*, **57**: 907–921.
- 380 Chow, N., and James, N.P. 1987b. Cambrian Grand Cycles : A northern Appalachian perspective  
381 Cambrian Grand Cycles : A northern Appalachian perspective. Geological Society of  
382 America Bulletin, **98**: 418–429.
- 383 Cowan, C.A., and James, N.P. 1993. The interactions of sea-level change, terrigenous-sediment  
384 influx, and carbonate productivity as controls on Upper Cambrian Grand Cycles of western  
385 Newfoundland, Canada. Geological Society of America Bulletin, **105**: 1576–1590.
- 386 Derry, L.A., Kaufman, A.J., and Jacobsen, S.B. 1992. Sedimentary cycling and environmental  
387 change in the late Proterozoic: evidence from stable isotopes. *Geochimica et Cosmochimica*  
388 *Acta*, **56**: 1317–1329.
- 389 Fan, R., Deng, S.H., and Zhang, X.L. 2011. Significant carbon isotope excursions in the Cambrian  
390 and their implications for global correlations. *Science China Earth Sciences*, **54**: 1686–1695.
- 391 Folk, R.L. 1951. Stages of textural maturity in sedimentary rocks. *Journal of Sedimentary*  
392 *Research*, **21**: 127–130.
- 393 Gilleadeau, G.J. and Kah, L.C., 2013. Carbon isotope records in a Mesoproterozoic spicratonic  
394 sea: Carbon cycling in a low-oxygen world. *Precambrian Research*, **228**: 85-101.
- 395 Glumac, B., and Walker, K.R. 1998. A Late Cambrian positive carbon-isotope excursion in the  
396 Southern Appalachians; relation to biostratigraphy, sequence stratigraphy, environments of

- 397 deposition, and diagenesis. *Journal of Sedimentary Research*, **68**: 1212–1222.
- 398 Gruszczynski, M., Halas, S., Hoffman, A., and Makowski, K. 1989. A brachiopod calcite record of  
399 the oceanic carbon and oxygen isotope shifts at the Permian/Triassic transition.
- 400 James, N.P., and Stevens, R.K. 1986. Stratigraphy and correlation of the Cambro-Ordovician Cow  
401 Head Group, western Newfoundland. *Geological Survey of Canada Bulletin*, **366**:143
- 402 Joachimski, M.M., Pancost, R.D., Freeman, K.H., Ostertag-Henning, C., and Buggisch, W. 2002.  
403 Carbon isotope geochemistry of the Frasnian-Famennian transition. *Palaeogeography*,  
404 *Palaeoclimatology, Palaeoecology*, **181**: 91–109.
- 405 Knight, I., and Boyce, W.D. 2009. The Reluctant Head Formation, Goose Arm Thrust Stack,  
406 Newfoundland Humber Zone: new observations on the stratigraphy, biostratigraphy and  
407 implications for the evolution of the Cambrian—Ordovician shelf. *Current Research:*  
408 *Newfoundland and Labrador Department of Natural Resources, Geological Survey Report*.
- 409 Kouchinsky, Bengtson, S., Gallet, Y., Korovnikov, I., Pavlov, V., Runnegar, B., Shields, G.,  
410 Veizer, J., Young, E., and Ziegler, K. 2008. The SPICE carbon isotope excursion in Siberia: a  
411 combined study of the upper Middle Cambrian–lowermost Ordovician Kulyumbe River  
412 section, northwestern Siberian Platform. *Geological Magazine*, **145**: 609–622.
- 413 Lavoie, D., Desrochers, A., Dix, G., Knight, I., and Hersi, O. 2012. The great American carbonate  
414 bank in eastern Canada: An overview. *AAPG Memoir 98 Great American Carbonate Bank*,  
415 **98**: 499–523.
- 416 Marengo, P.J., Corsetti, F.A., Kaufman, A.J. and Bottjer, D.J. 2008. Environmental and diagenetic  
417 variations in carbonate associated sulfate: An investigation of CAS in the Lower Triassic of  
418 the western USA. *Geochimica et Cosmochimica Acta* **72**, 1570–1582.
- 419 Moore, C.H. 2002. Carbonate Reservoirs Porosity Evolution and Diagenesis in a Sequence  
420 Stratigraphic Framework.
- 421 Neilson, J.E., Brasier, A.T. and North, C.P. 2016. Primary aragonite and high-Mg calcite in the late  
422 Cambrian (Furongian): Potential evidence from marine carbonates in Oman. *Terra Nova*, **28**:  
423 306-315.
- 424 Palmer, A.R. 1965. Trilobites of the Late Cambrian Pterocephaliid Biome in the Great Basin,  
425 United States. *United States Geological Survey Professional Paper*, **493**: 1–105.
- 426 Palmer, A.R., and James, N.P. 1979. The Hawke Bay event: A circum- Iapetus regression near the  
427 lower middle Cambrian boundary. *Virginia Polytechnic Institute & State University*.  
428 *Department of Geological Sciences. Memoir*, **2**: 15–18.
- 429 Patterson, W.P., and Walter, L.M. 1994. Depletion of  $^{13}\text{C}$  in seawater  $\Sigma\text{CO}_2$  on modern carbonate  
430 platforms: significance for the carbon isotopic record of carbonates. *Geology*, **22**, 885-888.
- 431 Paul, D., and Skrzypek, G. 2007. Assessment of carbonate-phosphoric acid analytical technique  
432 performed using GasBench II in continuous flow isotope ratio mass spectrometry.  
433 *International Journal of Mass Spectrometry*, **262**: 180–186.
- 434 Saltzman, M.R. 2002. Carbon and oxygen isotope stratigraphy of the Lower Mississippian  
435 (Kinderhookian–lower Osagean), western United States: implications for seawater chemistry  
436 and glaciation. *Geological Society of America Bulletin*, **114**, 96-108.
- 437 Saltzman, M.R., Cowan, C. a., Runkel, A.C., Runnegar, B., Stewart, M.C., and Palmer, a. R. 2004.  
438 The Late Cambrian Spice ( $^{13}\text{C}$ ) Event and the Sauk II-Sauk III Regression: New Evidence  
439 from Laurentian Basins in Utah, Iowa, and Newfoundland. *Journal of Sedimentary Research*,

- 440           **74**: 366–377.
- 441 Saltzman, M.R., Davidson, J.P., Holden, P., Runnegar, B., and Lohmann, K.C. 1995. No statistical  
442 support for sudden (or Sea-level-driven changes in ocean chemistry at an Upper  
443 Cambrian\extinction horizon. *Geology*, **23**: 893–896.
- 444 Saltzman, M.R., Ripperdan, R.L., Brasier, M.D., Lohmann, K.C., Robison, R.A., Chang, W.T.,  
445 Peng, S., Ergaliev, E.K., and Runnegar, B. 2000. A global carbon isotope excursion (SPICE)  
446 during the Late Cambrian: Relation to trilobite extinctions, organic-matter burial and sea  
447 level. *Palaeogeography, Palaeoclimatology, Palaeoecology*, **162**: 211–223.
- 448 Saltzman, M.R., Runnegar, B., and Lohmann, K.C. 1998. Carbon isotope stratigraphy of upper  
449 Cambrian (Steptoean stage) sequences of the eastern Great Basin: Record of a global  
450 oceanographic event. *Bulletin of the Geological Society of America*, **110**: 285–297.
- 451 Saltzman, M.R., Young, S. a, Kump, L.R., Gill, B.C., Lyons, T.W., and Runnegar, B. 2011. Pulse  
452 of atmospheric oxygen during the late Cambrian. *Proceedings of the National Academy of  
453 Sciences of the United States of America*, **108**: 3876–3881.
- 454 Schidlowski, M. 1992. *Early Organic Evolution: Implications for Mineral and Energy Resources.*  
455 *Edited by M. Schidlowski, S. Golubic, M.M. Kimberley, D.M. McKirdy, and P.A. Trudinger.*  
456 Springer-Verlag Berlin Heidelberg.
- 457 Scholle, P.A. 1977. Deposition, diagenesis, and hydrocarbon potential of deeper-water  
458 limestonesle. *In Short Course Notes. American Association of Petroleum Geologists,*  
459 Midland, TX
- 460 Schrag, D.P., Berner, R.A., Hoffman, P.F., and Halverson, G.P. 2002. On the initiation of a  
461 snowball Earth. *Geochemistry Geophysics Geosystems*, **3**: 1–21.
- 462 Sepkoski, J.J. 1982. Mass extinctions in the Phanerozoic oceans: a review. *Geological Society of  
463 America, Special Paper*, **190**: 283–289.
- 464 Sloss, L.L. 1963. Sequences in the cratonic interior of north America. *Bulletin of the Geological  
465 Society of America*, **74**: 93–114.
- 466 Spötl, C., and Vennemann, T.W. 2003. Continuous-flow isotope ratio mass spectrometric analysis  
467 of carbonate minerals. *Rapid Communications in Mass Spectrometry*, **17**: 1004–1006.
- 468 Westrop, S. 1992. Upper Cambrian (Marjuman-Steptoean) trilobites from the Port au Port Group,  
469 western Newfoundland. *Journal of Paleontology*, **66**: 228–255
- 470 Williams, H. 1976. Tectonic stratigraphic subdivision of the Appalachian Orogen.. *Geological  
471 Society of America, Abstracts with Programs*, **8**: 300.
- 472 Williams, H. 1979. Appalachian Orogen in Canada. *Canadian Journal of Earth Sciences*, **16**: 792–  
473 807.
- 474 Woods, M., Wilby, P., Leng, M., Rushton, A., and Williams, M. 2011. The Furongian (late  
475 Cambrian) Steptoean Positive Carbon Isotope Excursion (SPICE) in Avalonia. *Journal of the  
476 Geological Society*, **168**: 851–862.
- 477 Yochelson, E.L. 1984. The Biomere Problem: Evolution of an Idea. *Journal of Apleontology*, **59**:  
478 599-611.
- 479

480 **Table 1. Quartz grain size for March Point and Felix Cove sections.**

<b>Hight</b>	<b>March Point</b>		<b>Felix Cove</b>		
	<i>222.3 m</i>	<i>222.5m</i>	<i>23 m</i>	<i>23.4 m</i>	<i>24 m</i>
<b>Average</b>	88	89	473	466	456
<b>Maximum</b>	338	224	734	815	858
<b>Minimum</b>	37	36	116	227	138
<b>Median</b>	75	78	504	439	409
<b>n</b>	31	31	31	31	31

481

482 **Table 2. March point section isotopic results.**

<b>Sample description</b>	<b>Sample height (m)</b>	$\delta^{13}\text{C}_{\text{org}}$ (‰)**	<b>%C</b>	$\delta^{13}\text{C}_{\text{carb}}$ (‰)*	$\delta^{18}\text{O}_{\text{carb}}$ (‰)*	<b>Laboratory</b>
Glauconitic grainstone	9.25	-		-0.96	-8.09	LAMIR
Grainstone	56.75	-		-1.79	-5.51	LAMIR
Grainstone	59.00	-		-1.32	-5.70	LAMIR
Grainstone	67.00	-		-0.41	-7.63	LAMIR
Grainstone	83.50	-		-1.80	-7.37	LAMIR
Grainstone	86.50	-		-1.26	-7.28	LAMIR
Grainstone	106.00	-		-2.46	-6.74	LAMIR
Grainstone	109.50	-		-3.84	-7.62	BGS
Grainstone interbedded with mudstone	115.25	-		-1.77	-6.55	LAMIR
Glauconitic grainstone	122.5	-29.2	0.2	-	-	BGS
Reddish grainstone interbedded with shale	126.00	-		-2.16	-8.01	LAMIR
Shale	132.50	-28.41	0.4	-	-	BGS
Shale	133	-27.9	0.3	-	-	BGS
Shale	133.50	-29.47		-	-	BGS
Grainstone interbedded with mudstone	136.25	-		-3.18	-7.38	BGS
Shale	136.5	-30.8		-	-	BGS
Grainstone interbedded with mudstone	137.00	-		-4.16	-7.57	LAMIR
Grainstone	140.25	-		-2.54	-8.19	LAMIR
Shale	145.00	-27.48	0.1			BGS

Glauconitic bioclastic grainstone	152.25	-		-1.29	-8.00	LAMIR
Glauconitic bioclastic grainstone	152.50	-		-0.82	-7.84	BGS
Shale	153.25	-28.71	0.1	-	-	BGS
Shale	154.25	-26.61	0.1	-	-	BGS
Shale	155.25	-27.50	0.1	-	-	BGS
Shale	157.25	-28.40	0.1	-	-	BGS
Shale	157.25	-28.70	0.1	-	-	BGS
Mudstone interbedded with shale	160.25	-26.68	0.3	-	-	BGS
Mudstone interbedded with shale	162.25	-27.07	0.1	-	-	BGS
Mudstone interbedded with shale	166.75	-26.79	0.04	-	-	BGS
Glauconitic grainstone	167.00	-		-0.90	-7.94	LAMIR
Glauconitic grainstone	167.50	-27.88	0.3	-	-	BGS
Glauconitic grainstone	167.75	-27.35	0.1	-	-	BGS
Mudstone	168.75	-27.82	0.3	-	-	BGS
Glauconitic grainstone	170.75	-28.01	1.9	-	-	BGS
Glauconitic grainstone interbedded with mudstone	174.00	-27.70	0.5	-	-	BGS
Glauconitic grainstone interbedded with mudstone	175.50	-		-1.16	-5.90	BGS
Mudstone	175.50	-27.97	0.2	-	-	BGS
Glauconitic grainstone interbedded with mudstone	176.50	-		-1.49	-6.72	LAMIR
Glauconitic grainstone interbedded with mudstone	176.50	-24.77	0.3	-	-	BGS
Parted limestone dolomitized	179.00	-		-0.84	-7.19	LAMIR
Dolomitized parted limestone	179.00	-		-0.82	-6.50	LAMIR
Dolomitized parted limestone	179.75	-25.67	0.4	-	-	BGS
Glauconitic grainstone	180.50	-27.36	2.1	-	-	BGS
Dolomitized oolitic grainstone	183.75	-30.02	0.2	-	-	BGS
Dolomitized oolitic grainstone	184.50	-		-1.72	-6.87	LAMIR
Dolomitized oolitic grainstone	189.50	-		-1.53	-6.56	LAMIR



Mudstone	194.00	-22.47	0.3	-	-	BGS
Dolomitized oolitic grainstone	194.25	-27.21	0.5	-	-	BGS
Dolomitized oolitic grainstone	194.75	-26.68	0.5	-	-	BGS
Dolomitized oolitic grainstone interbedded with mudstone	198.50	-28.24	0.1	-	-	BGS
Parted limestone	199.50	-28.55	0.04	-	-	BGS
Dolomitized oolitic grainstone	200.25	-		-1.61	-6.76	LAMIR
Dolomitized oolitic grainstone	201.50	-28.17	0.1	-	-	BGS
Dolomitized oolitic grainstone	206.00	-21.31	0.8	-	-	BGS
Dolomitized oolitic grainstone	208.00	-		-1.29	-6.66	LAMIR
Dolomitized oolitic grainstone	215.50	-		-0.68	-6.93	LAMIR
Dolomitized oolitic grainstone	218.50	-		-0.46	-5.27	BGS
Parted limestone	218.50	-22.55	0.5	-	-	BGS
Dolomitized oolitic grainstone	222.75	-		+1.13	-5.08	BGS
Dolomitized oolitic grainstone	223.60	-		+0.52	-4.58	BGS
Dolomitized oolitic grainstone	223.75	-		+0.79	-5.76	BGS
Parted limestone	224.75	-25.79	0.1	-	-	BGS
Parted limestone	225.50	-		-0.31	-4.75	BGS
Parted limestone	226.25	-		-0.18	-4.04	BGS
Parted limestone	226.25	-25.55	0.1	-	-	BGS
Parted limestone	226.75	-26.3	1.1	-	-	BGS
Glaucconitic grainstone	230.00			-1.74	-7.73	BGS
Glaucconitic grainstone	230.00	-26.24		-	-	BGS
Mudstone	230.75	-		-1.35	-8.18	BGS
Mudstone	231.50	-		-1.83	-8.47	BGS
Mudstone	233.50	-		-1.05	-7.95	BGS
Mudstone	235.00	-		-1.19	-8.08	BGS
Glaucconitic grainstone	236.00	-		-1.73	-8.32	BGS

Glauconitic grainstone	236.00	-	-1.67	-8.62	BGS
Glauconitic grainstone	236.75	-	-2.01	-7.86	BGS
Grainstone	239.25	-	-1.07	-6.57	LAMIR
Grainstone	239.25	-23.05	-	-	BGS
Dolomitized oolitic grainstone	244.50	-	-1.38	-3.32	LAMIR

483 \*Overall analytical reproducibility for  $^{13}\text{C}$  and  $^{18}\text{O}$  ( $1\sigma$ ): BGS - 0.1‰; LAMIR: not determined

484 \*\*Overall analytical reproducibility for  $^{13}\text{C}_{\text{org}}$  (1SD): BGS -  $\pm < 0.1\text{‰}$

485

486 **Table 3. Felix Cove section isotopic results.**

Sample description	Sample height (m)	$\delta^{13}\text{C}_{\text{org}}$ (‰)**	%C	$\delta^{13}\text{C}_{\text{carb}}$ (‰)*	$\delta^{18}\text{O}_{\text{carb}}$ (‰)*	Laboratory
Grainstone	1.00	-		-2.0	-7.3	BGS
Grainstone	6.50	-		-1.3	-5.9	BGS
Shale	9.00	-26.6	1.0	-	-	BGS
Grainstone	13.00	-		-1.2	-7.0	BGS
Grainstone	16.80	-		-1.2	-7.5	BGS
Shale	17.25	-26.4	0.1	-	-	BGS
Shale	17.50	-27.5	0.17	-	-	BGS
Dolomitized oolitic grainstone	19.00	-		-0.5	-6.5	BGS
Dolomitized oolitic grainstone	22.25	-		-1.1	-9.0	BGS
Dolomitized oolitic grainstone	23.40	-		+0.4	-5.4	BGS
Dolomitized oolitic grainstone	24.00	-		+0.9	-5.4	BGS
Dolomitized oolitic grainstone	24.00	-		+0.87	-5.55	BGS
Dolomitized oolitic grainstone	25.50	-		+0.8	-5.4	BGS
Dolomitized oolitic grainstone	26.00	-		+1.02	-5.57	BGS
Shale	26.60	-23.5	0.01	-	-	BGS
Dolomitized oolitic grainstone	27.25	-		+0.9	-5.7	BGS
Dolomitized oolitic grainstone	27.50	-		+1.59	-5.76	BGS
Dolomitized oolitic grainstone	29.75	-		+1.83	-5.34	BGS

Shale	30.75	-25.7	0.04	-	-	BGS
Shale	33	-25.0	0.04	-	-	BGS
Dolomitized oolitic grainstone	35.25	-		+1.70	-5.46	BGS
Shale	36.00	-26.1	0.19	-	-	BGS
Mudstone	36.50	-		+1.10	-5.30	BGS

---

487 \*Overall analytical reproducibility for  $^{13}\text{C}_{carb}$  and  $^{18}\text{O}$  ( $1\sigma$ ): BGS - 0.1‰

488 \*\*Overall analytical reproducibility for  $^{13}\text{C}_{org}$  ( $1\sigma$ ): BGS -  $\pm < 0.1\%$

489

490 **Figure 1. Record of the SPICE excursion and global chronostratigraphic framework (after**  
 491 **Saltzman et al. 2004).**

492 **Figure 2. Study area in the Port au Port Peninsula. Location of the logged sections are shown**  
 493 **by black rectangles: 1) March Point and 2) Felix Cove.**

494 **Figure 3. Schematic stratigraphic log of the Port au Port Group (after Chow, 1986). Each of**  
 495 **the Grand Cycles (A, B and C) consists of a lower shaley half-cycle mainly composed of**  
 496 **parted limestone (interbedded shale and mudstone) and an upper carbonate half-cycle of**  
 497 **oolitic grainstone / bioherms. Estimated Sauk II-III sequence limit is indicated (Chow and**  
 498 **James 1987b, Saltzman et al. 2004).**

499 **Figure 4. Outcrop photos of SPICE-bearing layers: (a) Felix Cove outcrop at 22.5 m showing**  
 500 **the massive sandstone (S) that overlies the thrombolite layer at 22.25 m. Some intervals in the**  
 501 **thrombolite contains vugs parallel to bedding that may also occur in the sandstone (arrow);**  
 502 **(b) Detail from Felix Cove of thrombolite at 22.25 m; (c) West Felix Cove outcrop with pillow**  
 503 **thrombolites (T) and the overlying sandstone (S); (d) Detail from March Point of columnar**  
 504 **stromatolite at 222.5 m; (e) Detail of the dolomitized glauconitic grainstone (DG) above the**  
 505 **stromatolite (STR); (f) View of the outcrop with the dolomitized glauconitic grainstone (DG)**  
 506 **overlying the stromatolite.**

507 **Figure 5. Felix cove section: (a) Photomicrograph of the sandstone at 22.5m (peak SPICE),**  
 508 **with quartz (Qz), crinoid bioclasts (Cr) and a few glauconite grains (G) and peloids (P),**  
 509 **cemented by calcite (pinkish stain), with minor dolomite replacement (uncrossed polarizers)**  
 510 **(b) Photomicrograph of the equivalent sandstone layer in West Felix Cove cemented by**  
 511 **dolomite replacing calcite (pinkish stain), with minor dolomite replacement (uncrossed**  
 512 **polarizers); March Point section: (c and d) Photomicrographs of dolomitized (D) glauconitic**  
 513 **(G) bioclastic (Cr) peloidal grainstone at 222.6m (peak SPICE). (d) Detail of the glauconite**  
 514 **(G) glauconite peloid partially replaced by dolomite (D) in (c); (e and f) Photomicrographs of**  
 515 **glauconitic (G) sandstone partially cemented by euhedral dolomite rhombs (D) at 226.5m.**

516 **Figure 6. Photomicrographs of March Point dolomitized layers. (a) Dolomitized grainstone at**  
 517 **189.5 m; (b) Dolomitized grainstone at 208 m with ghost of ooids (black arrows); (c)**  
 518 **Dolomitized grainstone at 215.5m; (d) Quartzose (Q) arenite cemented by dolomite (D) at**  
 519 **239.5 m.**

520 **Figure 7. March Point isotope results, showing  $\delta^{13}\text{C}_{\text{org}}$ ,  $\delta^{13}\text{C}_{\text{carb}}$  and  $\delta^{18}\text{O}_{\text{carb}}$  isotopic data.**  
 521 **Dolomitized samples indicated in red.**

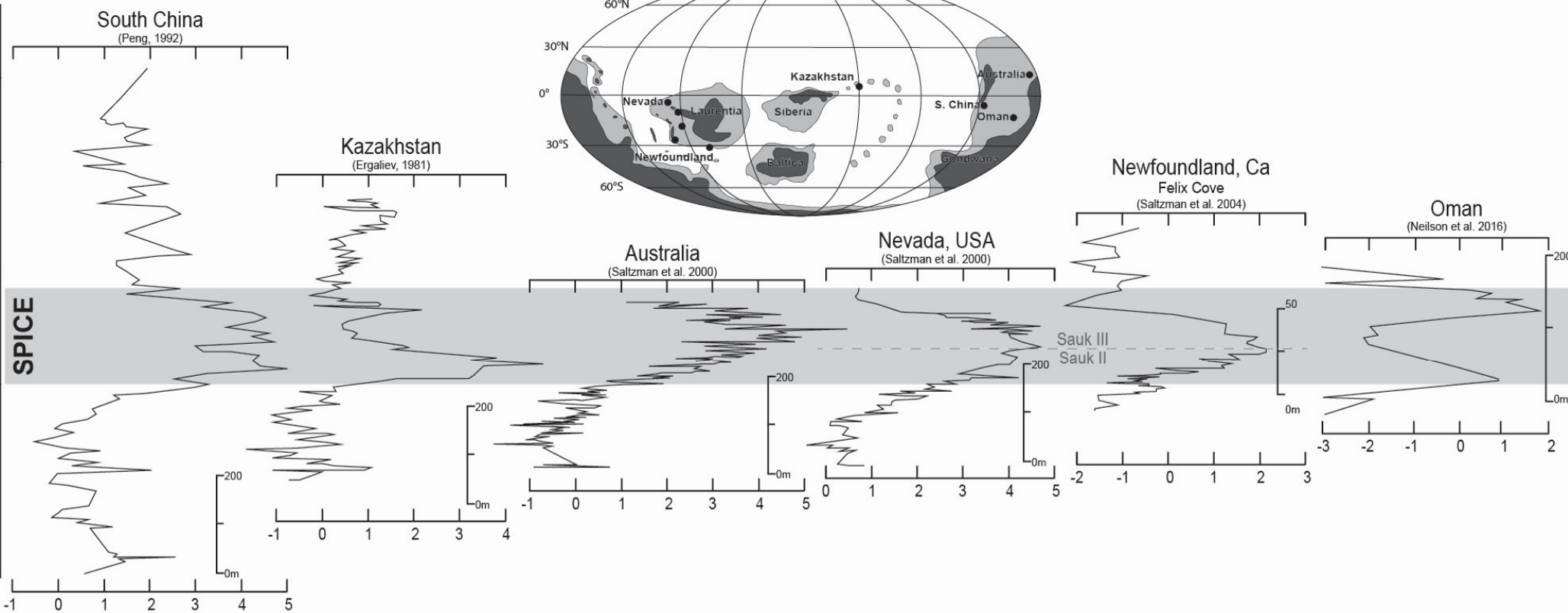
522 **Figure 8. Felix Cove isotope results, showing  $\delta^{13}\text{C}_{\text{org}}$ ,  $\delta^{13}\text{C}_{\text{carb}}$  and  $\delta^{18}\text{O}_{\text{carb}}$  isotopic data.**  
 523 **Dolomitized samples indicated in red.**

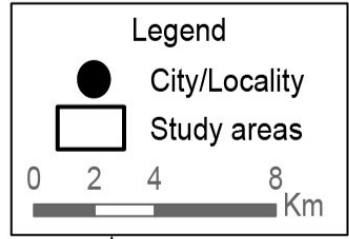
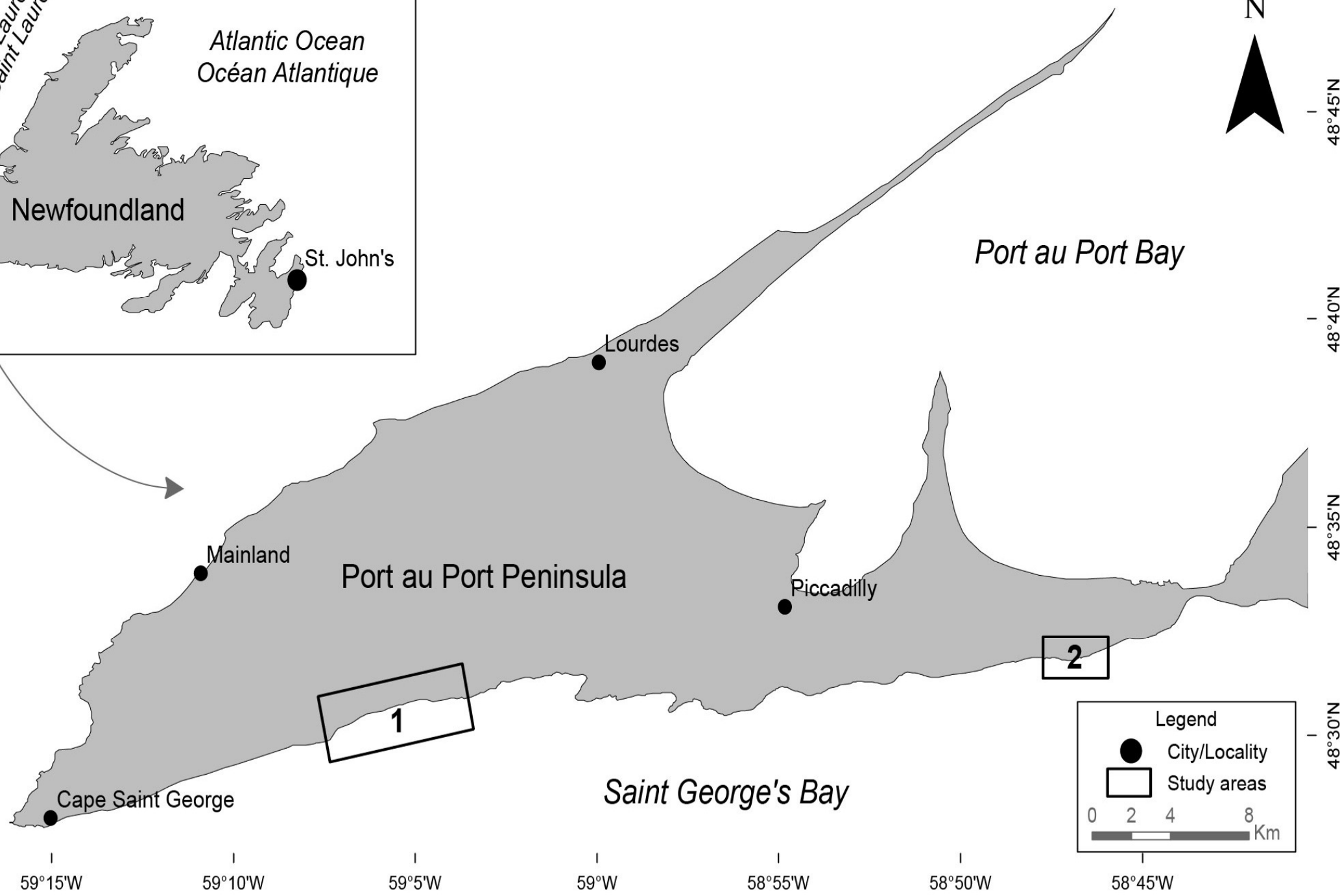
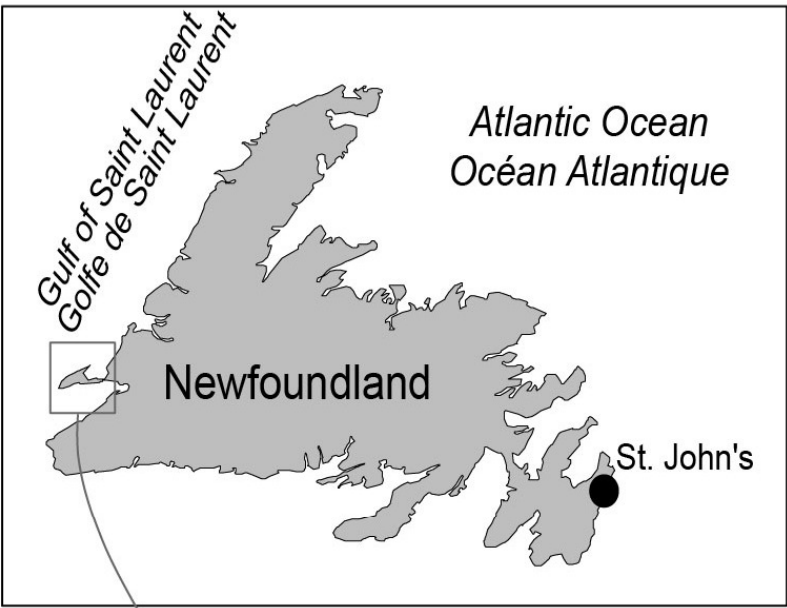
524 **Figure 9. Comparison between the expression of the SPICE in the March Point (1) and Felix**  
525 **Cove (2) sections. The grey shaded area indicates the correlation based on the carbonate**  
526 **carbon signature.**

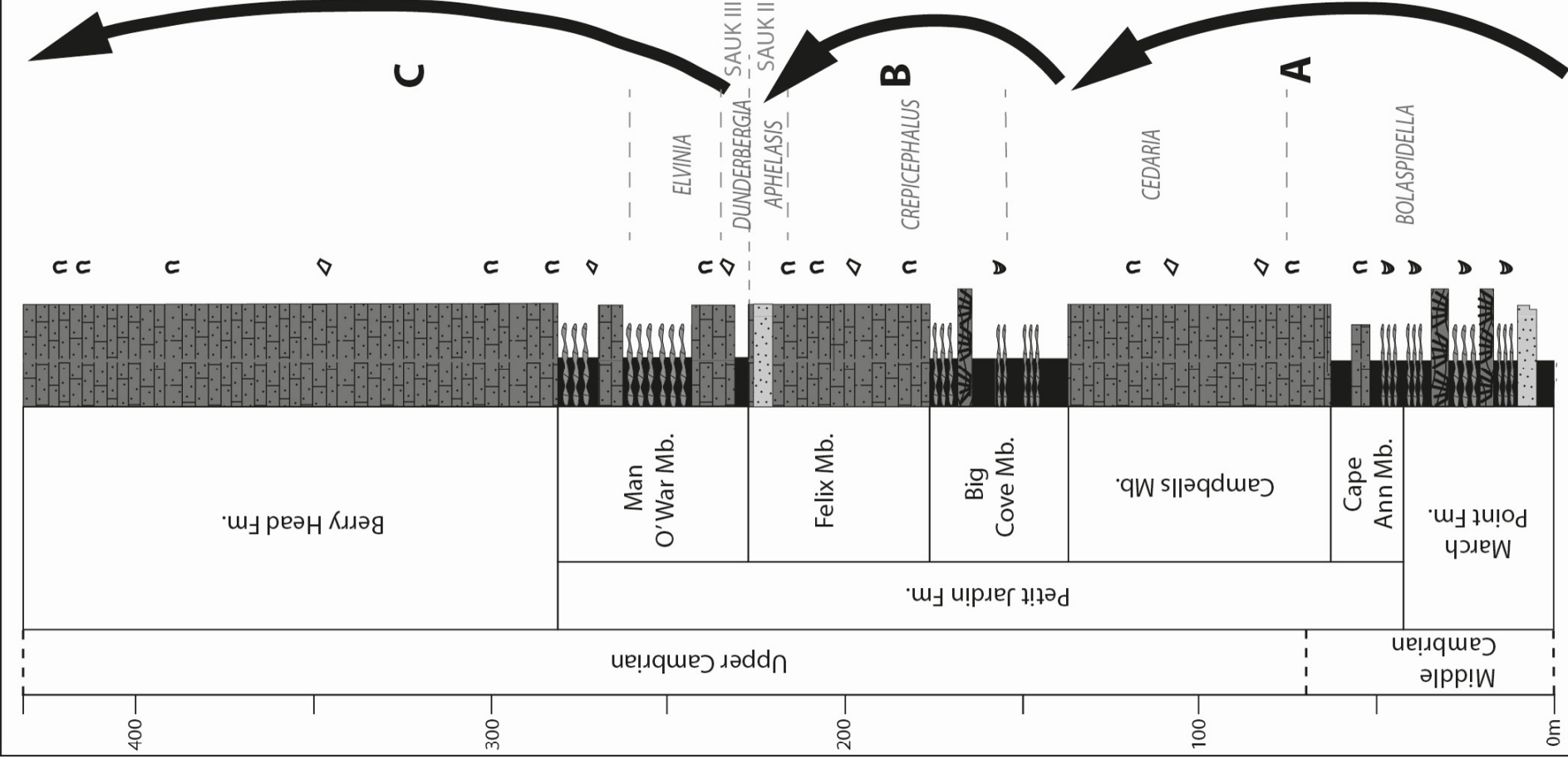
527 **Figure 10.  $\delta^{13}\text{C}_{\text{org}}$  and  $\delta^{13}\text{C}_{\text{carb}}$  data for A) March Point Sections and B) Felix Cove Section.**  
528 **The comparison between the curves shows a peak of organic excursion a few meters below**  
529 **(but nearly coincident with) the peak of the carbonate carbon excursion in the March Point**  
530 **section, while in Felix Cove both peaks occurs at same level.**

531 **Figure 11. Laurentia paleogeographic map (Blakey 2016), showing its evolution between 510**  
532 **Ma and 485 Ma. The red square indicates the position of western Newfoundland, yellow**  
533 **square indicates the position of southern Appalachians (Glumac and Walker 1998), and black**  
534 **squares indicates the positions of other SPICE localities in the United States (Nevada, Utah,**  
535 **Iowa and Minnesota) (Saltzman 2004). Detail of Newfoundland (NF) paleogeography and**  
536 **paleolatitudes are indicated on the map.**

Global Chronostratigraphy			
Age (Ma)	Series	Stage	Laurentian Stage
489	Furongian	Jiangshanian <sup>1c</sup>	Surwaptan
494		Paibian	Steptoean
497	Epoch 3	Guzhangian	Marjuan



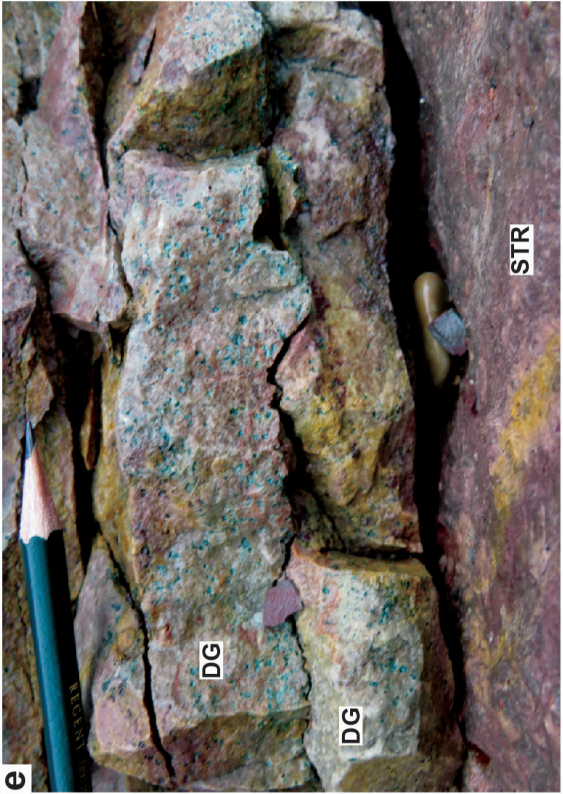
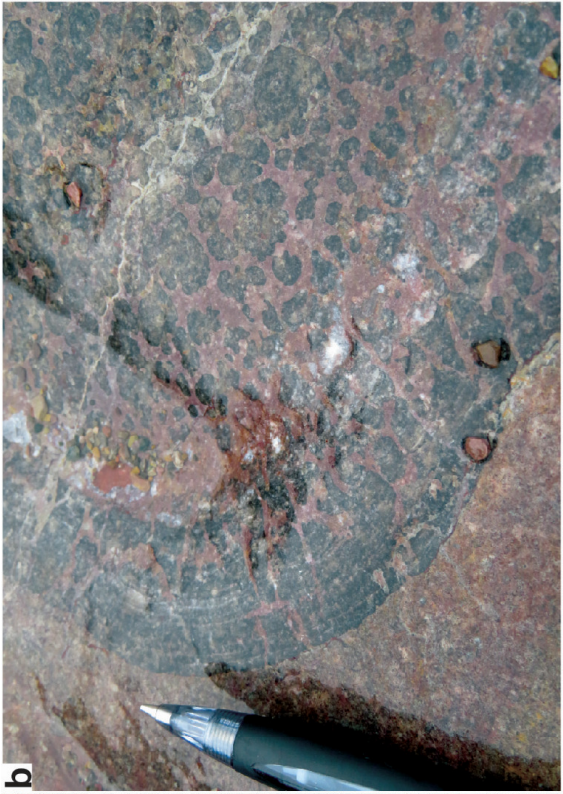


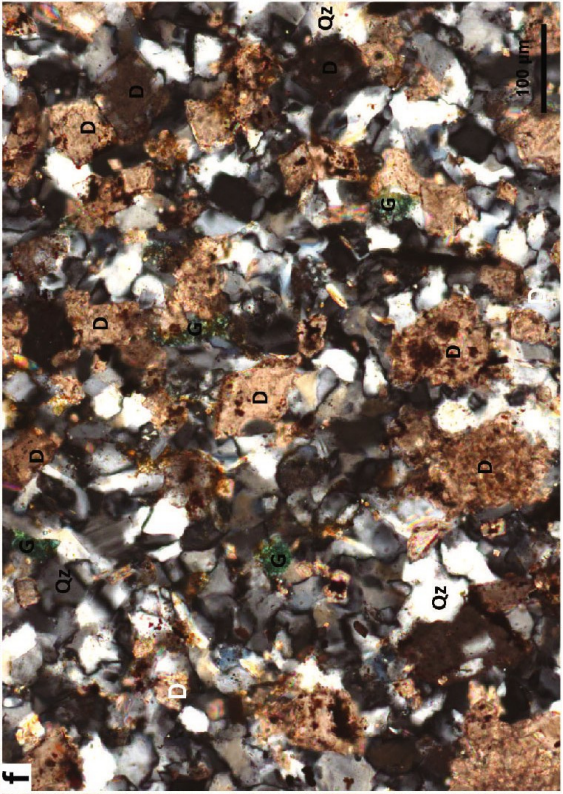
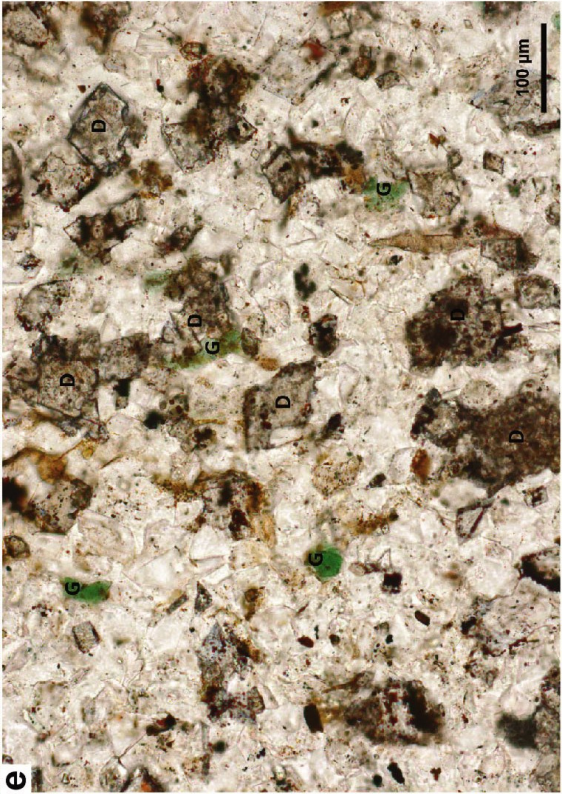
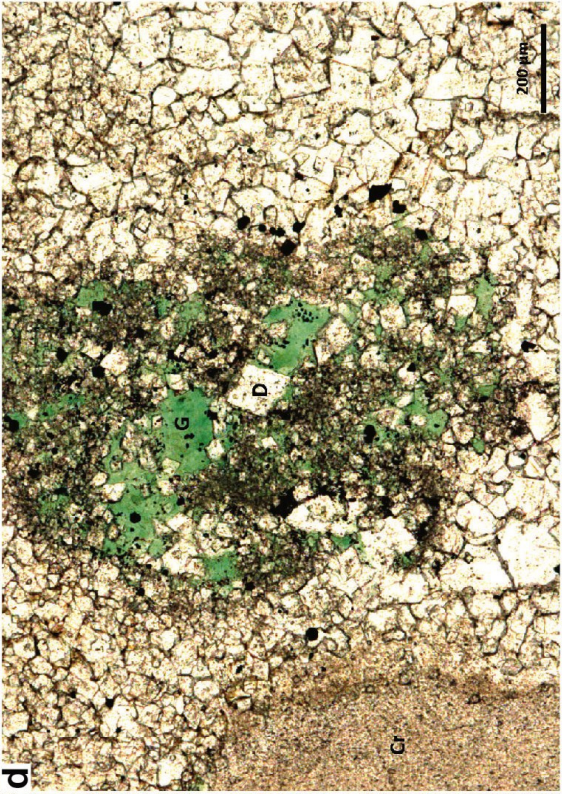
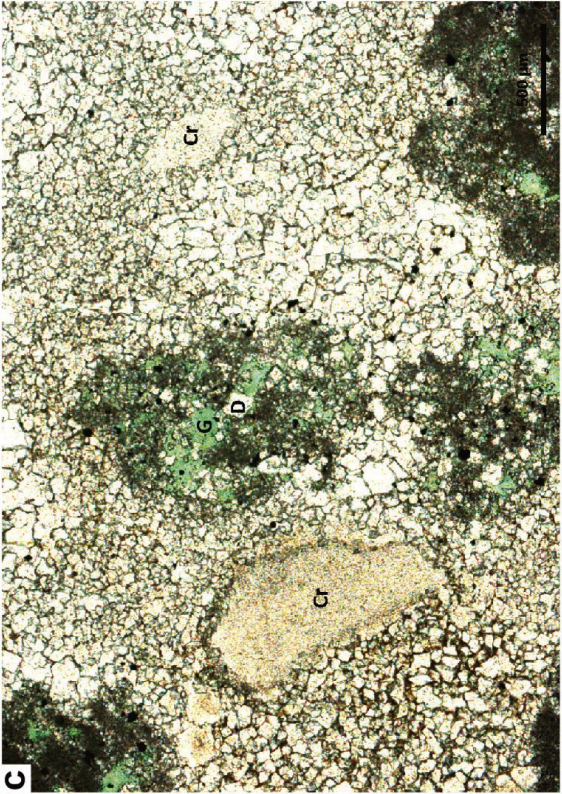
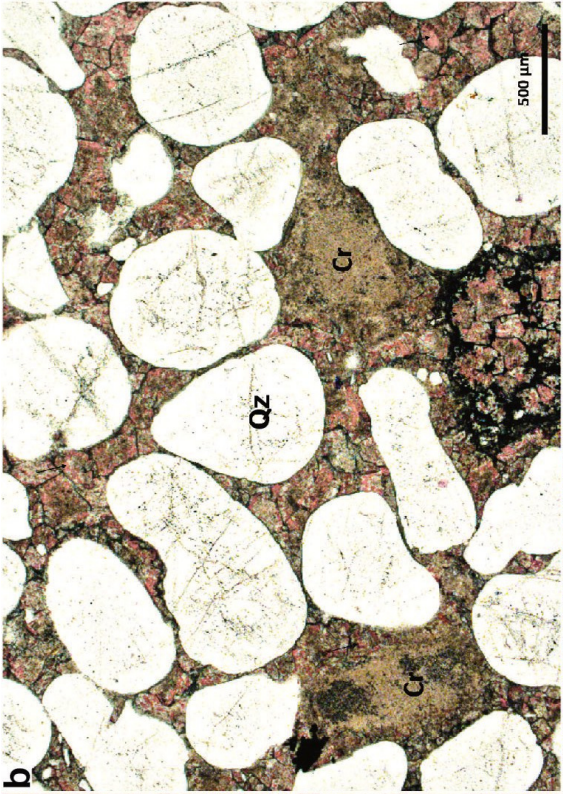


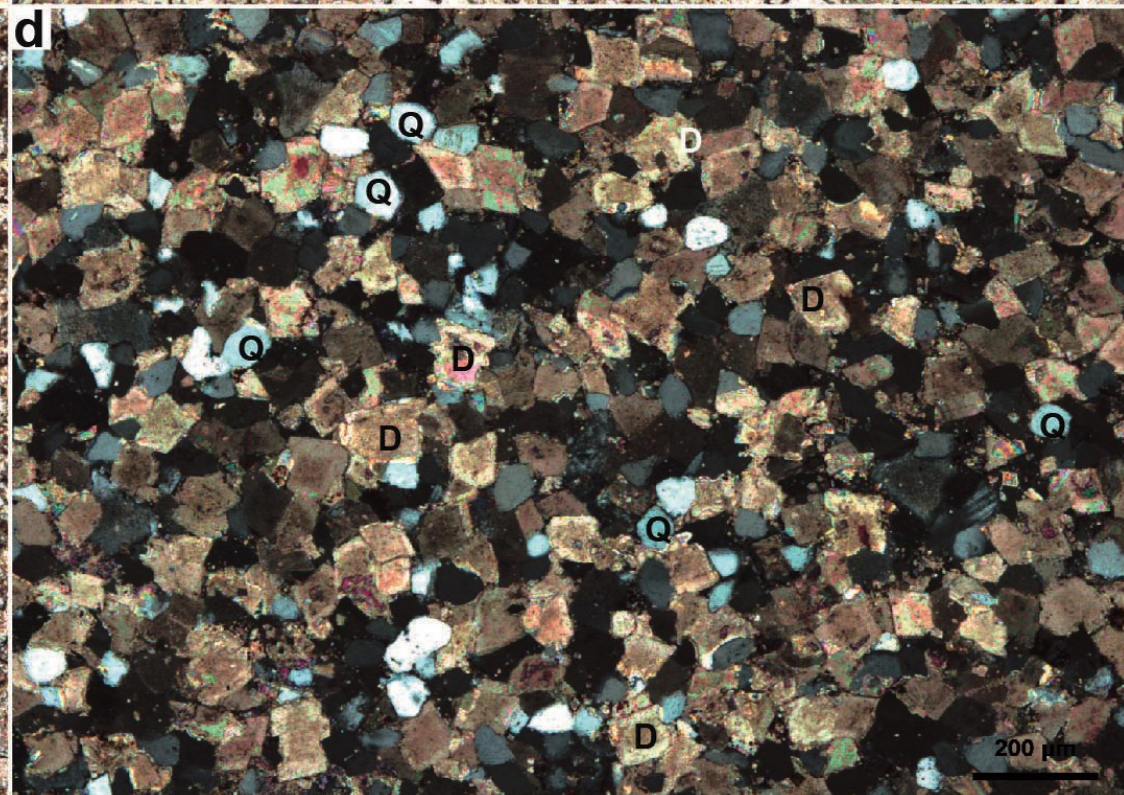
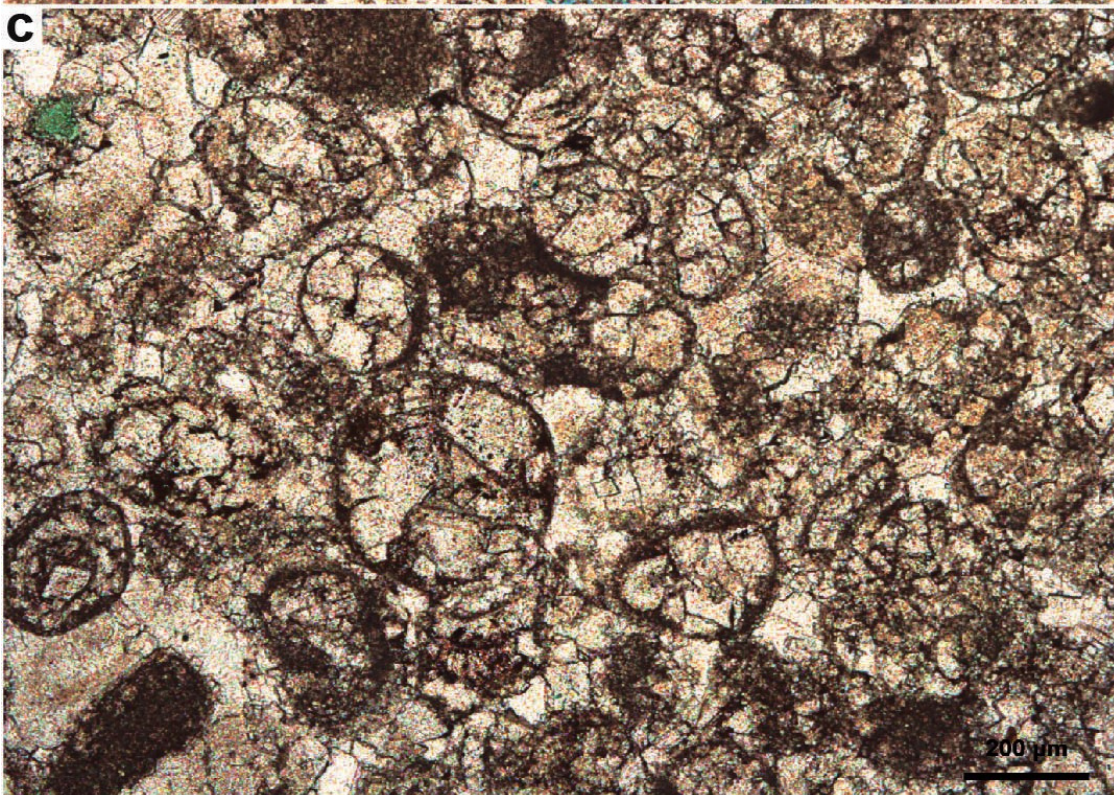
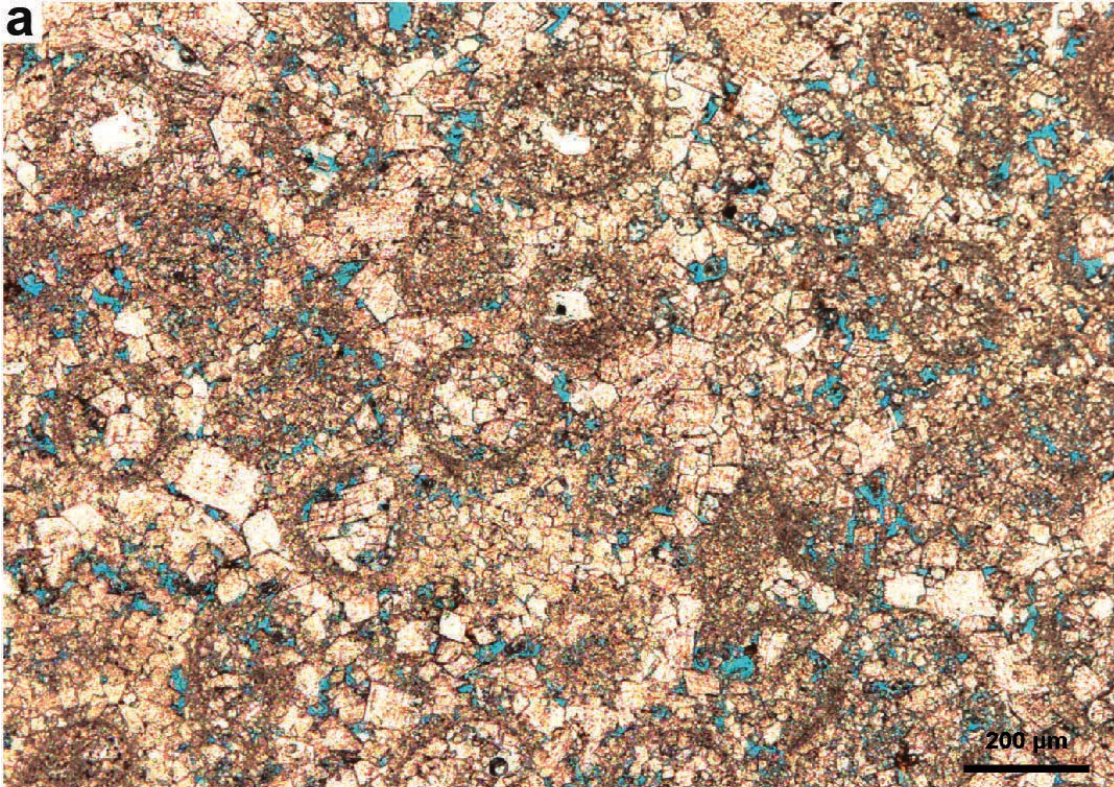
**LEGEND**

	GRAINSTONE		INTRACLASTS
	PARTED LIMESTONE		FLAT PEBBLES
	SHALE		BIOHERMS
	SANDSTONE		BIOTURBATION

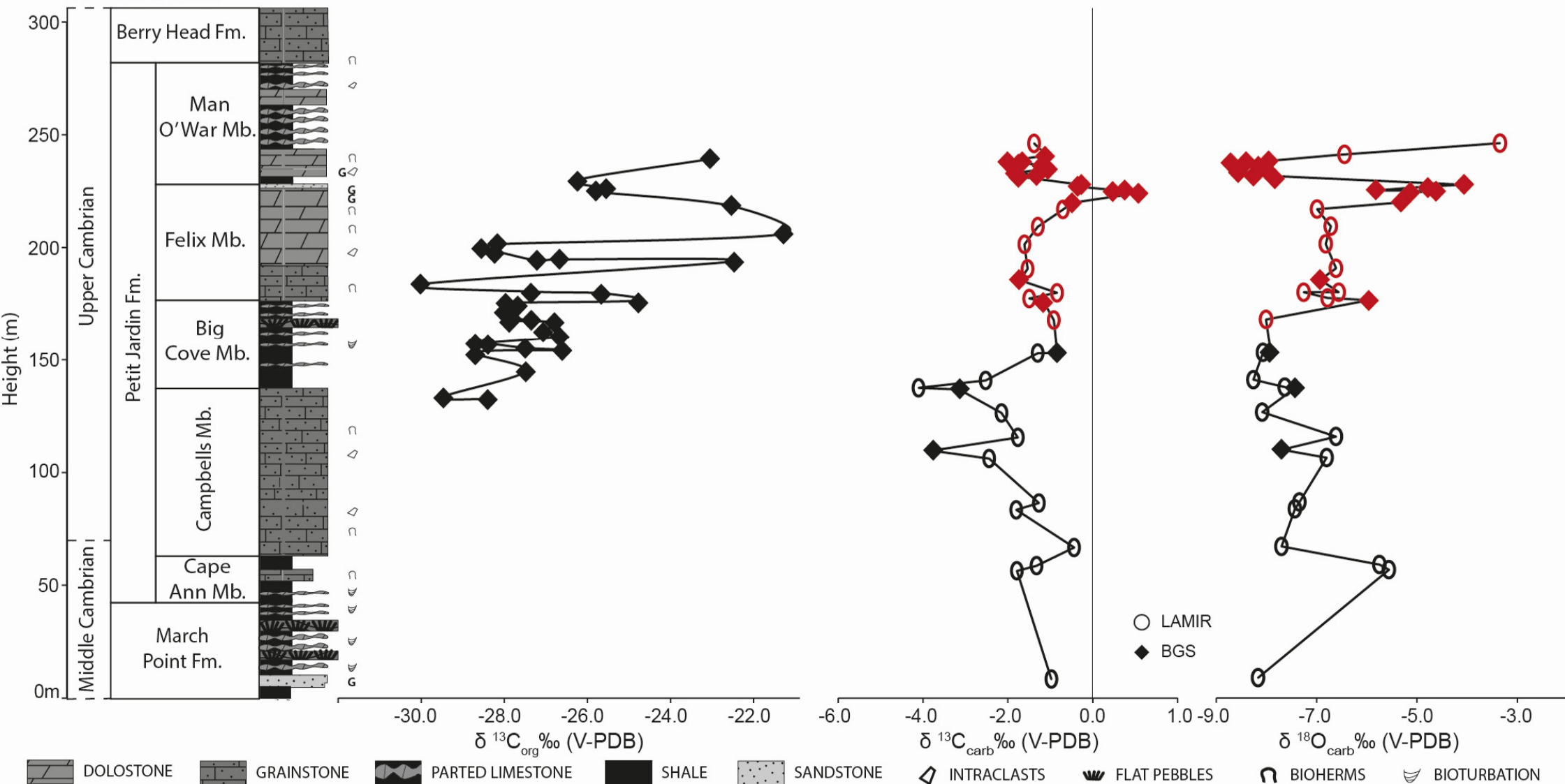




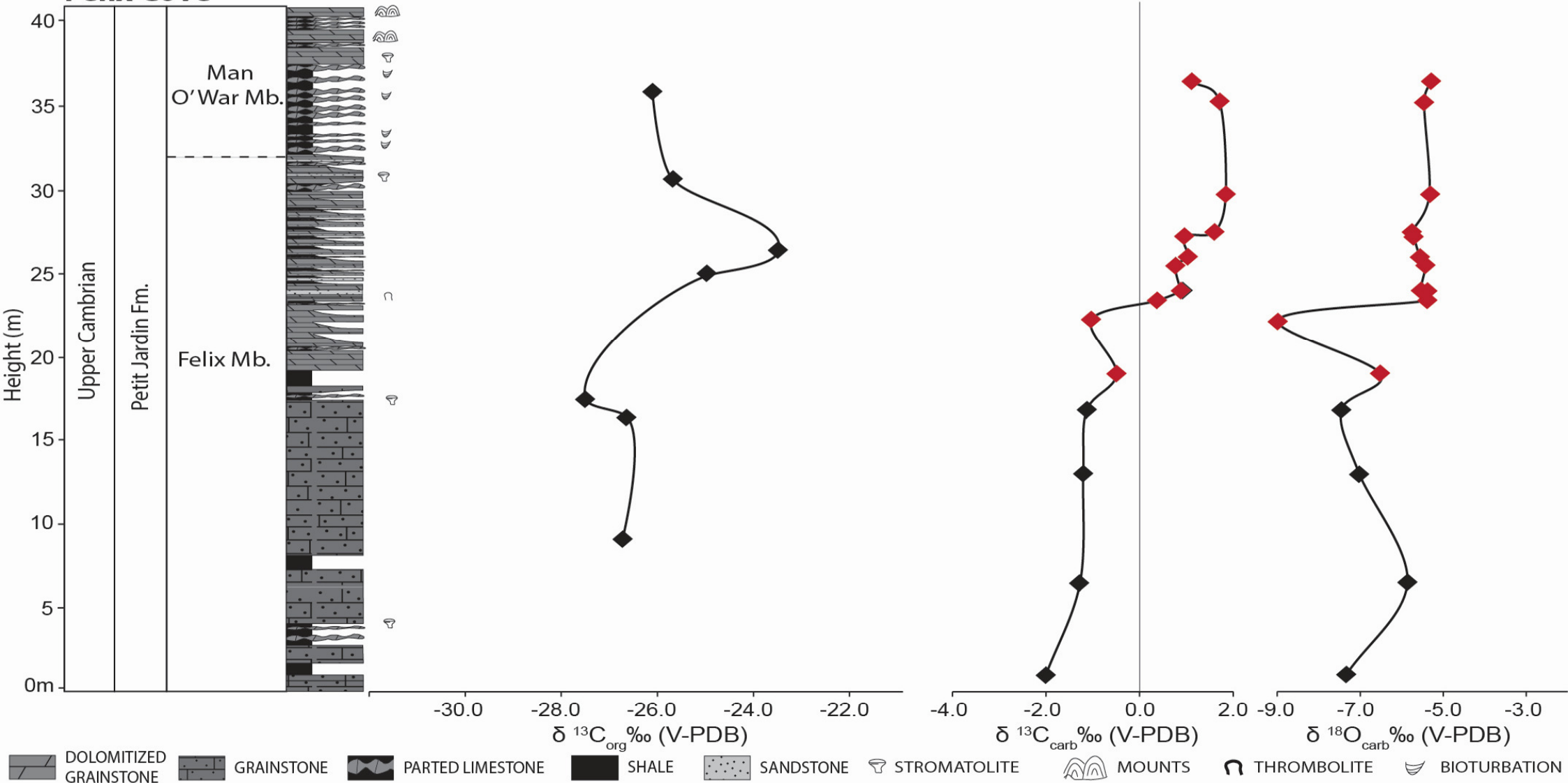




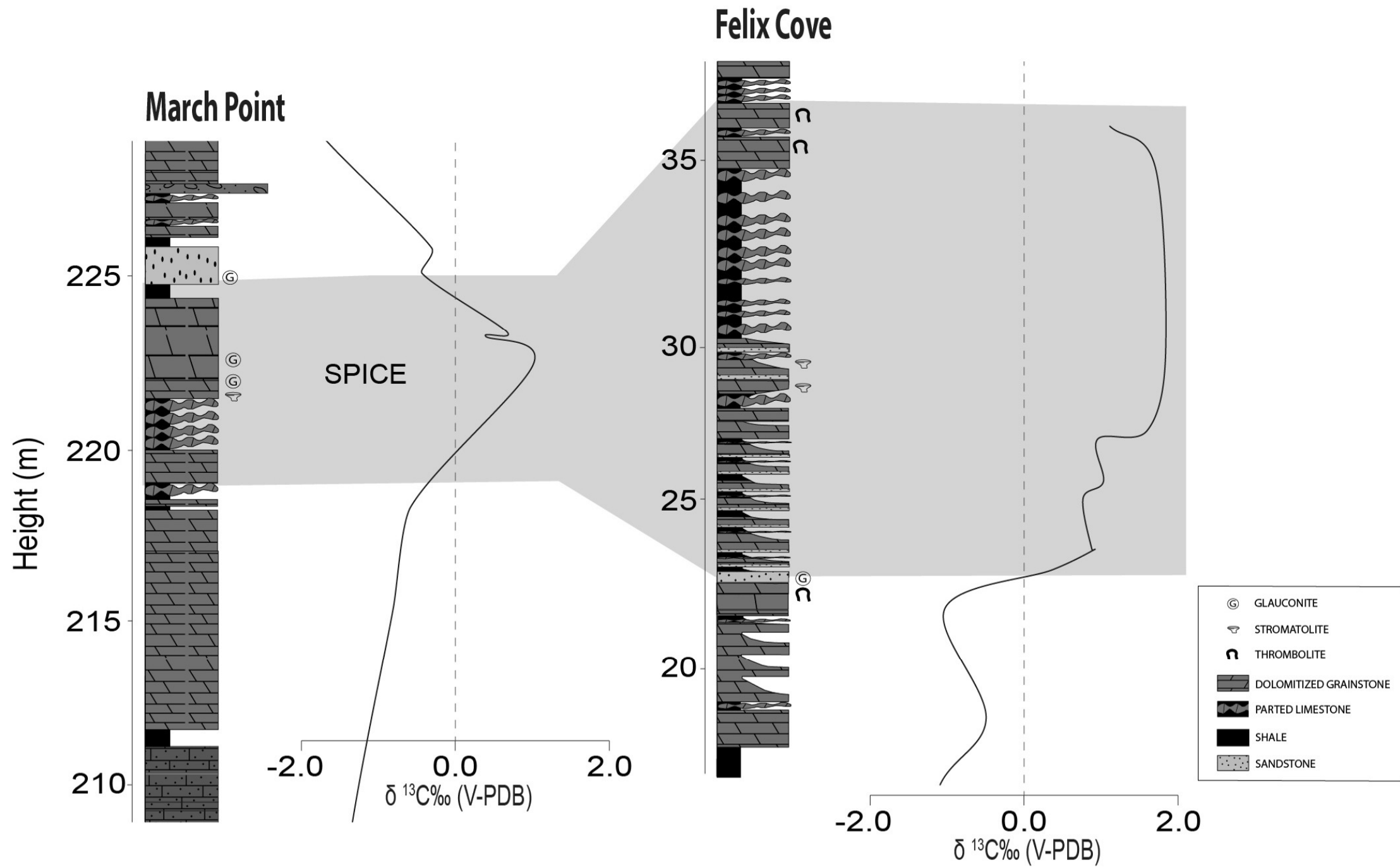
# March Point

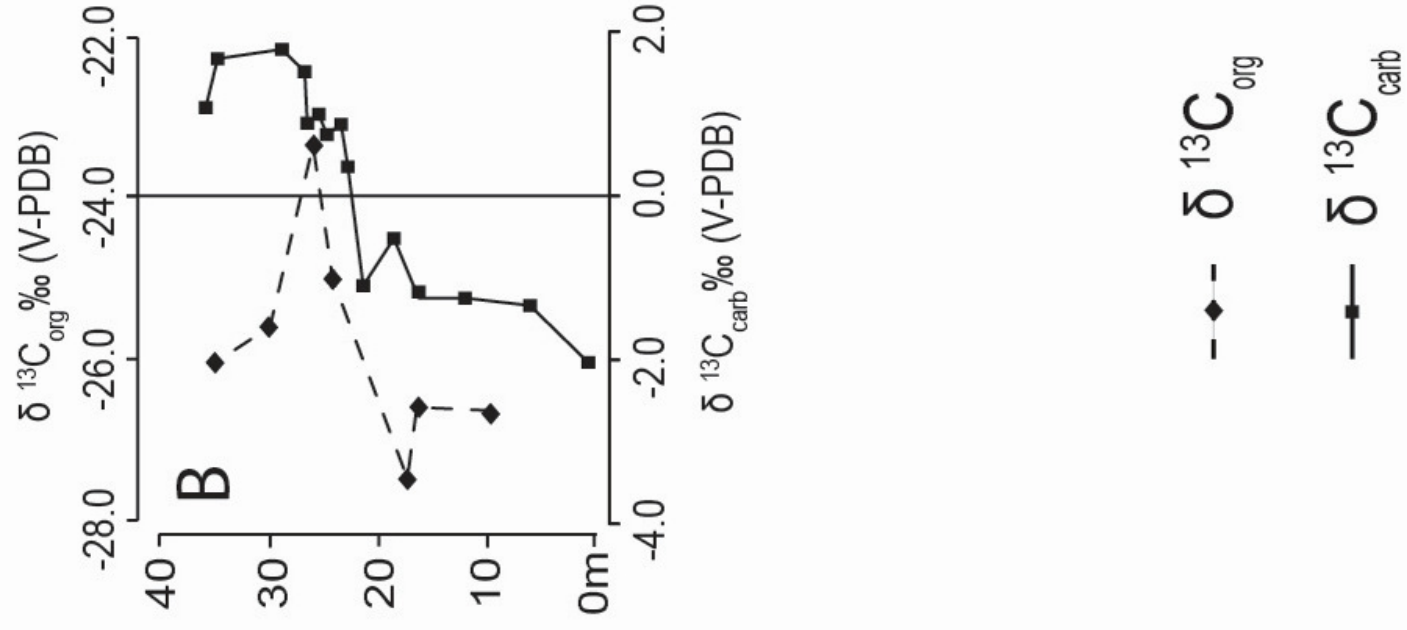
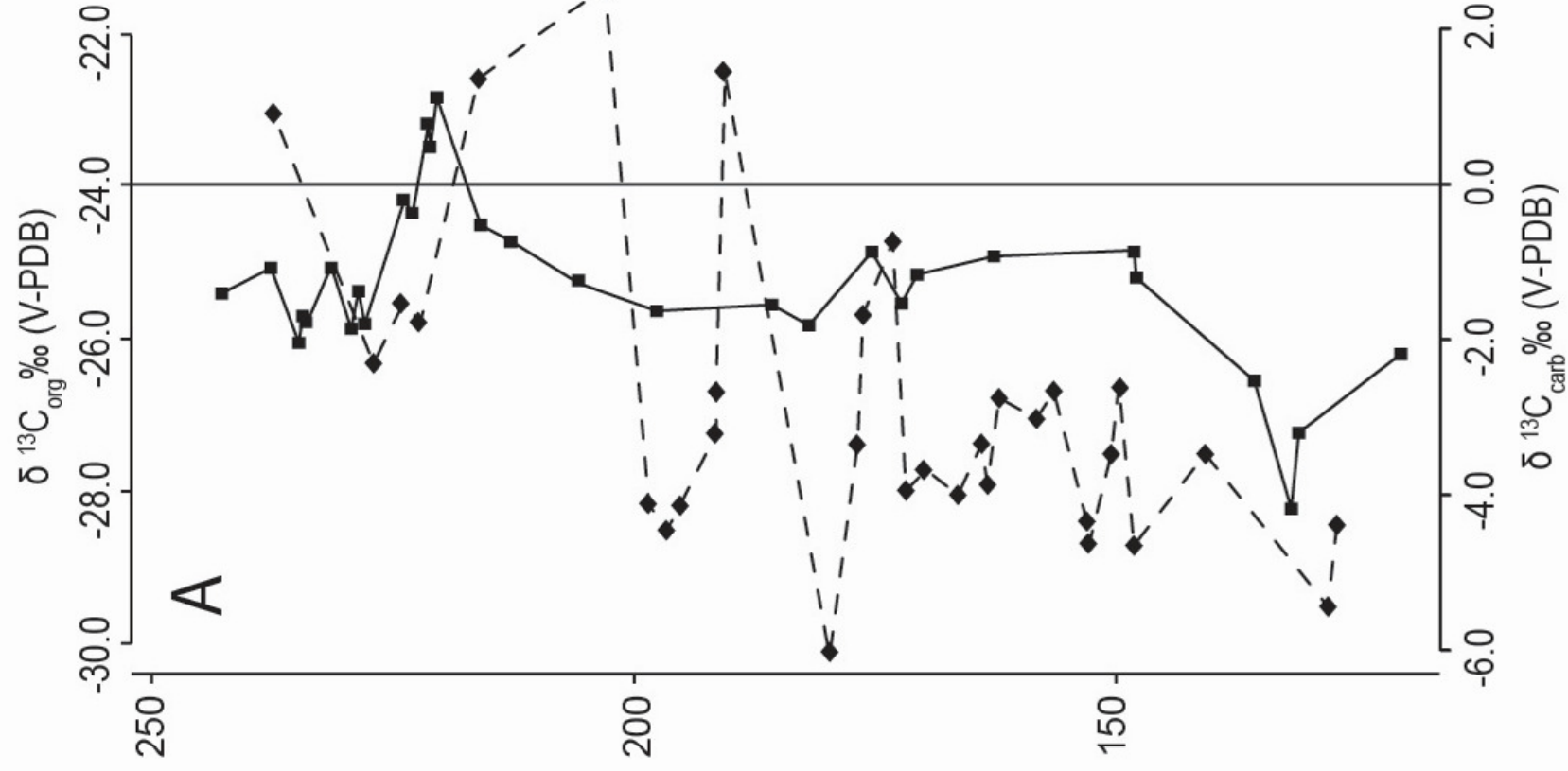


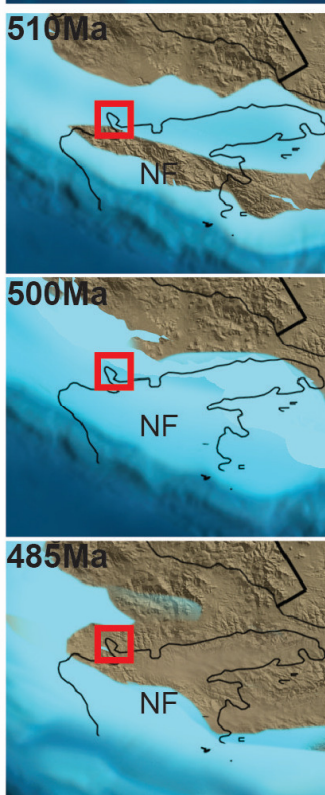
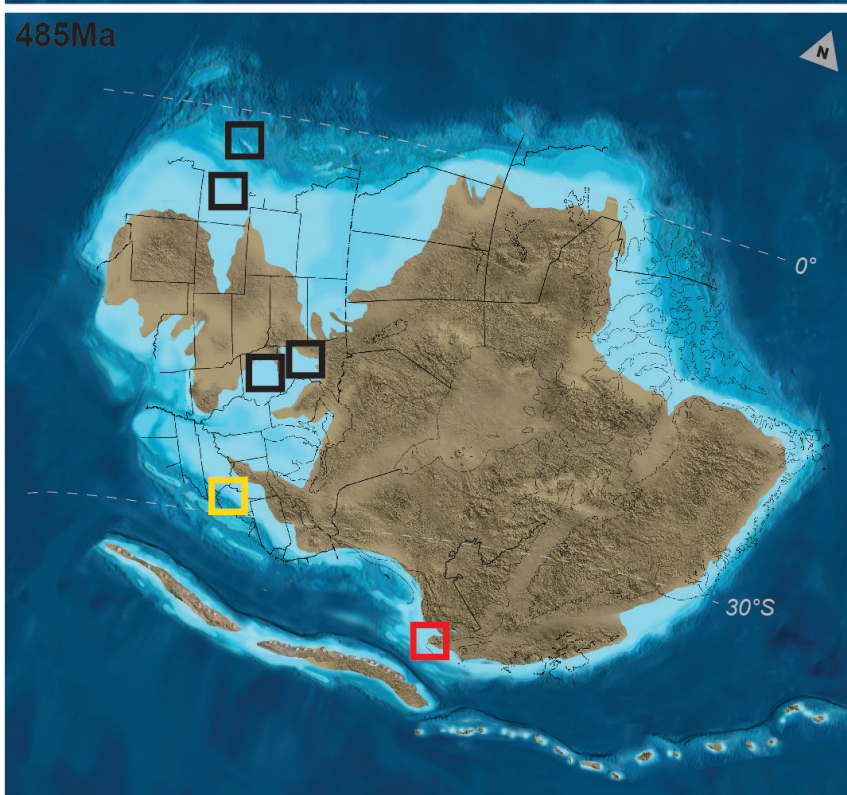
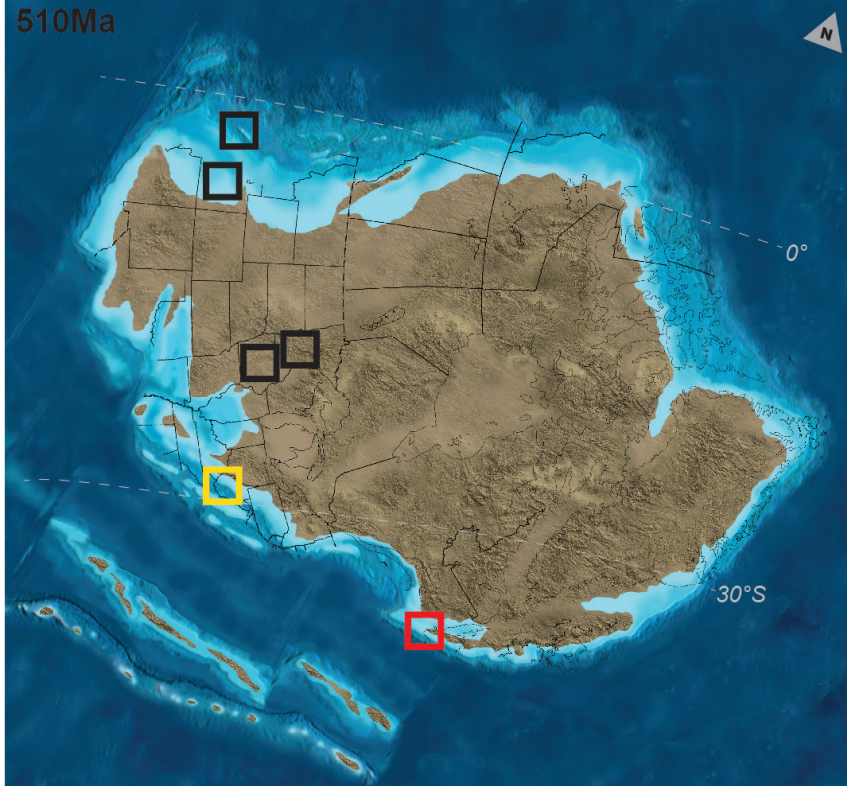
# Felix Cove



DOLOMITIZED GRAINSTONE  
  GRAINSTONE  
  PARTED LIMESTONE  
  SHALE  
  SANDSTONE  
  STROMATOLITE  
  MOUNTS  
  THROMBOLITE  
  BIOTURBATION










Detail of Newfoundland Paleogeography

Legend

- SPICE in Laurentia
-  Great America Carbonate Bank (Saltzman, 2004)
-  South Appalachians (Glumac and Walker, 1998)
-  This study